UNCERTAINTIES IN THE SOLUTIONS TO BOUNDARY ELEMENT METHOD: AN INTERVAL APPROACH

by

BARTLOMIEJ FRANCISZEK ZALEWSKI

Submitted in partial fulfillment of the requirements

For the degree of Doctor of Philosophy

Dissertation Adviser: Dr. Robert L. Mullen

Department of Civil Engineering

CASE WESTERN RESERVE UNIVERSITY

August, 2008

CASE WESTERN RESERVE UNIVERSITY

SCHOOL OF GRADUATE STUDIES

We hereby approve the thesis/dissertation of

_____Bartlomiej Franciszek Zalewski_____

candidate for the Doctor of Philosophy degree *.

(signed)_____Robert L. Mullen_____
(chair of the committee)

_____Arthur A. Huckelbridge_____

_____Xiangwu (David) Zeng_____

_____Daniela Calvetti_____

_____Shad M. Sargand_____

(date) _____4-30-2008_____

*We also certify that written approval has been obtained for any proprietary material contained therein.

With love I dedicate my Ph.D. dissertation to my parents.

TABLE OF CONTENTS

LIST OF TABLES

LIST OF FIGURES

ACKNOWLEDGEMENTS

My deepest expression of gratitude is directed toward my Ph.D. advisor Professor Robert L. Mullen for his advice and support throughout my doctoral program. Professor Mullen has not only allowed me to grow in research but also imparted the appreciation for the numerical and interval analysis. For all his commitment and dedication I will forever be indebted to him. I would like to thank my parents, Miroslawa and Krzysztof, and sister Alicja for their support throughout my education because without them many things would not be possible. I want to thank Professor Arthur A. Huckelbridge, who was my M.S. advisor, for all his help and support throughout my academic career. I am very grateful to Professor Mehdi Modares, who will always be my mentor and a good friend, for all his support, seemingly endless discussions, and collaboration. I want to thank my committee members, Professor Daniela Calvetti, Professor David Zeng, and Professor Shad Sargand for their support of this work. Many thanks go to Professor Rafi L. Muhanna for his support and involvement in this project, Professor Ivo Babuška for many of his insights, Professor Dario Gasparini whose every course helped me in better understanding engineering, and to Professor Adel Saada for many of his advices and lessons. Last but not least I thank my good friend Gregory G. Koscik for all the support throughout many years. I am very thankful to all the Professors, colleagues, students, and staff at Case Western Reserve University who made my educational experience a very pleasant and memorable one. Many thanks go to any other persons whom I met throughout the different stages of life who directly or indirectly contributed to my growth, all of whom I cannot name. Thank you.

LIST OF SYMBOLS

a – scalar

a_i – vector

a^* – Green's function

$\tilde{a}$ – interval number

$\tilde{a}_e$ – element of an interval vector

A – nxn matrix

$\tilde{A}$ – nxn interval matrix

$\tilde{A}_e$ – element of an interval matrix

b – $nx1$ vector

$\tilde{E}$ – interval bounds on an error

$f(\tilde{a})$ – interval valued function

I – identity matrix

n – normal vector

$q_{singular}$ – singular value of a variable

R – remainder of Taylor series

w – weighted residual function

Γ – boundary of a system

ε – small finite number

ε_{ij} – small deformation strain tensor

Ω – domain of a system

π – constant ≈ 3.14

σ_{ij} – Green stress tensor

$\Phi(x)$ – interpolation function

ξ – source point location

A^{-1} – inverse operator on nxn matrix A

$\tilde{A}^{H}$ – hull inverse of nxn matrix $\tilde{A}$

$abs(..)$ – absolute value

max(..) – maximum value

$mid(\tilde{a})$ – mid-point of $\tilde{a}$

min(..) – minimum value

Uncertainties in the Solutions to Boundary Element Method: An Interval Approach

Abstract

By

BARTLOMIEJ FRANCISZEK ZALEWSKI

Interval boundary element method (IBEM) is developed allowing computation of the worst case behavior of the system due to numerical errors on the point-wise variable level. Three sources of error due to numerical analysis are considered; 1) errors occurring due to numerical integration, 2) errors occurring due to floating point number truncation, and 3) errors occurring due to the discretization of the integral equation resulting from boundary element formulation. The impact of uncertainty in the applied boundary conditions was also examined.

Boundary element method is a technique used to solve partial differential equations. This numerical scheme obtains approximate solutions which have been shown to converge on the global scale. However, the accuracy of the solutions on the local level has not been studied and needs to be considered for reliable engineering analysis. This work obtains the enclosure of the boundary integral equations, which result from boundary element formulation, via interval methods. The interval boundary integral equations are then solved using the conventional boundary element procedure. The resulting is the enclosure of the true solution of the boundary values. Form the worst case

bounds on the boundary values the worst case bounds in the domain of the problem are computed.

Interval analysis is used to treat errors due to numerical integration and floating point number truncation. An illustrative numerical scheme is considered to demonstrate the formulation and the rounding error is accounted for in the iterative scheme used to solve the resulting interval linear system of equations. The treatment of uncertainty in the boundary conditions is explored using interval concepts resulting in exact worst case bounds for the boundary values.

Chapter I

Introduction

Chapter I introduces the research topic and provides a brief historical background.

1.1 Background

In engineering, partial differential equations are used to model the behavior of systems such as heat transfer, electric conduction, fluid flow, acoustic wave propagation, and stress distribution. However, most of the partial differential equations cannot be solved exactly due of the complexity arising from satisfying a correct set of applied boundary conditions for geometry of any complexity. Many methods, such as finite element method (FEM), finite difference method (FDM), finite volume method (FVM), mesh free methods such as element free Galerkin (EFG) and natural element method (NEM), and discrete element method (DEM) have been developed to obtain approximate solutions to partial differential equations. Boundary element method (BEM) is a technique for obtaining approximate solutions to partial differential equations, in which the true solution is approximated by a polynomial interpolation. Unlike the more widely used FEM, BEM requires that only the boundary of the system is discretized; therefore, the dimension of the problem is reduced by one. In general, this allows for the decrease in computational time necessary to mesh the system or to refine an existing mesh. The dimension reduction characteristic of BEM makes it a very attractive computational tool for design engineers who must consider many system geometries.

In boundary element analysis (BEA) the mesh reduction, from domain of the system to the boundary of the system, is performed by transforming the domain variables to the variables on the boundary of the domain. The variable transformation is constructed using fundamental solutions of the governing partial differential equation, or Green's functions. Therefore, boundary element formulation is limited to partial differential equations for which the fundamental solution exists. Assuming that Green's function is known, the boundary integral equations are transformed using point collocation methods, where source points are located sequentially at all boundary nodes that map the domain variables such that they coincide to their nodal values. The boundary integral equations are then discretized into boundary elements and expressed in terms of a linear algebra problem. As in FEM, boundary elements consist of nodes and assumed polynomial interpolation between them. Since, in general, the polynomial interpolation is not the true solution to the integral equation; errors are introduced due to discretization of the problem.

In solving partial differential equations using any numerical method, one has to be aware that these techniques provide approximate solutions. The behavior of the errors in numerical methods has been studied (Babuška et al. 1986, Babuška and Strouboulis 2001) for the finite element method. In FEM the domain of the system is discretized into elements, for which a solution is assumed to be a polynomial interpolation between calculated discrete values. Assuming no other errors are present besides the discretization error, the solutions obtained using displacement based finite element method are the most optimal solutions in a given error norm to the original partial differential equation;

therefore, the norm of the solution converges to the true solution monotonically. Numerous error estimates have been made for finite element solution norms and energy norms both on a global and local scale. Global error estimates have been made using the L_2 norm as well as other norms showing the convergence of the solution. Element-wise estimates showed that the finite element solution approaches the true solution with mesh refinement. The convergence of the finite element solution has also been shown with increasing order of the polynomial approximation. In FEM, the discretization errors are always orthogonal to the approximate solutions; therefore, the error estimates smooth out the errors over the considered region and thus they do not give a good indicator of the point-wise behavior of the error. This is especially true for the global estimates where the error is estimated for the entire system and the behavior of the error within the system is unknown. Furthermore, the computation of there error estimates may become computationally expensive. In order to decrease the computational expense of computing error estimates for the original problem, error estimates of the dual problem have been made (Oden and Carey 1983, Oden and Prudhomme 2001), whose uniqueness is guaranteed by the Lax-Milgram Theorem (Lax and Milgram 1954). The dual problem is formulated by relating the error to the residual. This approach is justified since the residual contains all the information that is present in the numerical error. Same limitations of the error estimates of the dual problem as for the primal problem are present.

Finite difference method (Pilkey and Wunderlich 1994) is another technique for solving partial differential equations, in which the differential operator has been

approximated by a difference operator. FDM is often developed by the use of Taylor series expansion (Taylor 1715) which allows the study of the truncation error resulting from the truncation of the Taylor series in finite difference formulation. In finite difference method, the differential equation is approximated by a difference equation whose accuracy depends on the order of the polynomial of the assumed solution. Since the polynomial series is truncated, the remainder of the Taylor series provides an order of the error in the solution. As in the finite element method, the behavior of the finite difference error on the point-wise level for the entire domain is unknown and only an accuracy estimate of the solution can be obtained. The estimate of the discretization error in boundary element method has also been shown to decrease with element size (Cartensen and Stephan 1995, Dehao and Longhua 2005, Jou and Liu 1999, Rencis and Jong 1989); however, the equivalent problems associated with error estimates, not being able to predict point-wise behavior, apply.

Modern technology has allowed replacing the traditional verification techniques, i.e. experimental methods, with computational science (Babuška et al. 2007). This step is largely due to the continuous increase in the computational power of the modern day computers. As more engineering analyses are performed using numerical techniques, there arises a need for reliable computing methods. The traditional computational methods are incapable to address any perturbation of the original engineering system such as uncertainty in boundary conditions and/or system's parameters, as well as the perturbation of the solutions due to numerical errors imbedded in machine computations such as rounding and integration error. Moreover, the conventional error estimates, global

and local, are incapable of predicting the true discretization error on a point-wise, or design variable, level. Although error estimates describe the global behavior of the error, whether it is in the solution norm or energy norm, the guaranteed bounds on the true discretization error have thus far not been computed.

The objective of this research is to address the impact of the discretization error on the solution on the point-wise level. Considering the discretization error itself, and not its estimate, allows one to obtain the behavior of the error at every point in the domain of the system. Since the discretization error can only be computed if the true solution is known, computing the discretization error for a general problem is not possible. In this work interval methods are studied to guarantee the enclosure of the true solution within a convex closed set of real numbers or an interval number. This work, to the author's knowledge, is the first to quantify the worst case discretization error on the point-wise level. Other aspects impacting the numerical solution on the local variable level such as integration error, arising from numerical integration of the kernel functions, rounding error, occurring due to truncation of the floating point numbers caused by limited machine precision, and uncertainty in boundary conditions are addressed and quantified using interval analysis. Interval analysis was chosen to handle the errors and uncertainties in the system due to its very elegant and computationally efficient nature as well as its versatility in considering all aspects of uncertainty in the solutions in an integrated fashion. The result of the research is a development of the interval boundary element method (IBEM) that is capable of considering the effect of the discretization error, integration error, rounding error, and uncertain boundary conditions on the point-wise

variable level. The IBEM formulation requires a development of a new method for enclosing integral equations, interval kernel splitting technique (IKST), and a new algorithm for solving interval linear system of equations. The methodology is computationally efficient and attractive due to its simplistic nature.

1.2 Overview

The dissertation is organized as follows. Chapter I provides historical background of BEA and interval analysis. Chapter II introduces the boundary element formulation for the Laplace equation. Chapter III demonstrates the applications of the boundary element method in engineering mechanics problems such as torsion problem and elasticity problem. Chapter IV reviews set-theoretic or interval mathematics. The author's major contributions are presented starting with chapter V, which describes the developed algorithms for solving interval linear system of equations. Chapter VI is devoted to the treatment of unknown but bounded boundary conditions. Chapter VII describes the integration and rounding errors and their treatment through interval approach. Chapter VIII introduces the discretization error in BEA. Chapter IX describes the bounding of the boundary integral equation by a kernel splitting technique. Chapter X is devoted to the treatment of the discretization error through an interval approach and provides a parameterized algorithm used to obtain nearly sharp error bounds on the point-wise boundary values. Chapter XI describes the special treatment of the bounds on the discretization error in the presence of geometrically induced singular flux solutions. Chapter XII treats the enclosure of the solution in the domain of the problem. Chapter

XIII contains example problems demonstrating effectiveness of the proposed method. Chapter XIV provides concluding remarks on the work.

1.3 Historical Background

1.3.1 Historical Background of Boundary Element Method

The use of numerical techniques to solve differential equations dates back to Leibnitz (1646-1716) but it's not until 1940 that the first estimate of the a-posteriori error was made (Babuška and Strouboulis 2001, Ostrowski 1940). Boundary element method is rooted to the formulation of integral equations that can be traced to Somigliana who derived forms of the integral solution identities based on the fundamental solutions for the elasticity problem (Somigliana 1885). The existence of the solutions and the discretization procedure for integral equations was demonstrated by Fredholm (Fredholm 1903) resulting in Fredholm equations of the first and second kind. Kellogg obtained a functional constraint between boundary values and normal derivatives of the harmonic functions by taking the source point in the domain of the system to the boundary of the system (Kellogg 1929). In 1965 Kupradze introduced vector integral equations in the concept of elasticity problems (Kupradze 1965) and in 1967 Rizzo developed numerical solutions for the two-dimensional elasticity problem using boundary integral equations (Rizzo 1967). The name boundary integral equation (BIE) was officially given by Sweldow and Cruse in their work on three-dimensional elastostatics (Sweldow and Cruse 1971). In 1977 Jaswon and Symm published the first book on integral equation methods for numerical solutions to boundary value problems in potentials and elasticity (Jaswon

and Symm 1977). The term boundary element originated in the Department of Civil Engineering at Southampton University and first appeared in Brebbia's work on potential problems (Brebbia 1977). In 1978 the first book on boundary element method was published (Brebbia 1978). Mansur and Brebbia computed elastodynamic problems using boundary elements (Brebbia et al. 1983) and Rencis and Mullen developed a self-adaptive mesh refinement for the elasticity problem and for the Laplace equation (Rencis and Mullen 1986, Rencis and Mullen 1988). Mullen and Rencis have studied iterative methods for solving linear system of equations resulting from boundary element formulation (Mullen and Rencis 1987). The integration error estimate was considered by Sawaga (Sawaga 1986) and the estimate of the discretization error was studied (Cartensen and Stephan 1995, Dehao and Longhua 2005, Jou and Liu 1999, Rencis and Jong 1989).

1.3.2 Historical Background of Interval Analysis

The concept of interval analysis is dated back to Archimedes of Syracuse, 287-212 BCE, who bounded π by inscribing and circumscribing a circle with 12-sided, 24-sided, 48-sided, and 96-sided polygons. Using an iterative scheme, Archimedes bounded π by an interval $\left[3\frac{1}{7}, 3\frac{10}{71}\right]$ (Archimedes translated by Sir Thomas Health 1987). In modern times, the theory of interval algebra had been formulated by Sunaga (Sunaga 1958) and error analysis was first performed in digital computing (Collins 1960). Moore further studied interval error analysis (Moore 1962) and in 1965 the interval arithmetic in matrix approach was developed by Hansen (Hansen 1965). Hansen's methods were the first to obtain bounds on the solution to the interval linear system of equations. The first

interval analysis book has been published in 1966 by Moore (Moore 1966). The iterative scheme for the nearly sharp enclosure of the solution to interval linear system of equations has been formulated by Krawczyk (Krawczyk 1969). The enclosure of real roots using iterative methods was studied by Hansen (Hansen 1978). Rump (Rump 1980) improved the convergence of the iterative methods by introducing epsilon inflation. The solutions to interval linear equations have been further studied by Gay (Gay 1982). Overestimation in the solution to the interval linear system of equations has been considered by Neumaier (Neumaier 1987) and the sensitivity analysis for the systems of linear and nonlinear equations has developed by Rump (Rump 1990). Jansson considered interval linear system of equations for symmetric and skew-symmetric matrices (Jansson 1991) and obtained sharp bounds for those types of systems using a modified Krawczyk iteration. The interval application to mechanics was first considered in finite element method with the development of the fuzzy finite element method (FFEM) and the interval finite element method (IFEM) to treat uncertain loading conditions, material uncertainties, uncertain geometry, and rounding error for static problems (Muhanna and Mullen 1995, Muhanna and Mullen 1999, Muhanna and Mullen 2001, Mullen and Muhanna 1995, Mullen and Muhanna 1999, Mullen and Muhanna 2002). Interval treatment of system uncertainty in IFEM was extended in the dynamic analysis using interval response spectrum analysis (IRSA) (Modares and Mullen 2004) and structural system stability (Modares et al. 2005). Penalty based approach for IFEM considering uncertainty in material characteristics for skeletal elements was developed (Muhanna et al. 2005) providing sharp bounds on the solution. Global optimization techniques were used to obtain sharp bounds for large system uncertainties in truss structures (Neumaier

and Pownuk 2007, Skalna and Pownuk 2008). Neumaier also provided theoretical bounds for the discretization errors and parameter uncertainties for linear elliptic partial differential equations (Neumaier 2007). The use of interval analysis in boundary element method can be traced to the treatment of uncertain boundary conditions through fuzzy approach (Burczynski and Skrzypczyk 1997). The resulting fuzzy linear system of equations is solved directly resulting in unrealistic and naïve bounds on the true solution. The interval treatment of uncertain systems has been made (Piasecka Belkhayat 2007) considering a constant but bounded system parameters. Considering constant system properties on the entire domain of the system is unrealistic and results in trivial formulation.

Chapter II

Boundary Element Analysis of Laplace Equation

Chapter II demonstrates the boundary element formulation for a liner elliptic partial differential equation with both Dirichlet and Neumann boundary conditions applied on the boundary of the system.

2.1 BEA Formulation for Laplace Equation

The boundary element formulation is described in literature (Aliabadi 2002, Beskos 1989, Brebbia 1978, Brebbia and Dominguez 1992, Hall 1994, Hartmann 1989, Liggett and Liu 1983, Linkov 2002, Pilkey and Wunderlich 1994, and Wrobel 2002). The following section is a review of the boundary element formulation for a linear elliptic partial differential equation. The equation that is used to demonstrate the procedure is the Laplace equation. The Laplace equation is:

$$\left.\begin{aligned} &\nabla \cdot (k\,\nabla u) = 0 \quad \textit{in } \Omega \\ &u = \hat{u} \quad \textit{on } \Gamma_1 \\ &k\frac{\partial u}{\partial n} = q = \hat{q} \quad \textit{on } \Gamma_2 \\ &\bigcup_{i=1}^{2} \Gamma_i = \Gamma \quad \textit{and} \quad \bigcap_{i=1}^{2} \Gamma_i = 0 \end{aligned}\right\} \tag{2.1}$$

where Ω is the domain of the system, Γ is the boundary of the system, where $\Gamma = \partial\Omega$, u is the value of the potential with a known Dirichlet, or forced, boundary condition of $\hat{u}$ on the boundary Γ_1, q is value of the flux with a known Neumann, or natural,

boundary condition of $\hat{q}$ on the boundary Γ_2, n is the outward unit normal vector to the boundary of the system, and k is the material property such as heat conductivity in heat transfer. In this work a constant material property is considered. It is assumed that at every point on the boundary either the Dirichlet or the Neumann boundary condition is known and that the boundaries Γ_1 and Γ_2, which do not intersect, form a closed boundary Γ. The solution to Laplace equation, in general, cannot be obtained directly and therefore an approximate method has to be used. The first step in approximation of the equation is to express it in a weighted residual form, also known as the weak form:

$$\int_{\Omega} \nabla^2 u w d\Omega = \int_{\Gamma_2} (q - \hat{q}) w d\Gamma_2 - \int_{\Gamma_1} (u - \hat{u}) \frac{\partial w}{\partial n} d\Gamma_1 \tag{2.2}$$

where w is the weighted residual function or the test function. To decrease the smoothness requirements on the solution, Eq. (2.2) is integrated by parts. This procedure is performed twice to obtain a non-symmetric weak form which has weaker smoothness requirements than a symmetric weak from used in the finite element formulation. After integration by parts is performed twice, Eq. (2.2) is rewritten as:

$$\int_{\Omega} \nabla^2 w u d\Omega = -\int_{\Gamma_2} \hat{q} w d\Gamma_2 - \int_{\Gamma_1} q w d\Gamma_1 + \int_{\Gamma_2} u \frac{\partial w}{\partial n} d\Gamma_2 + \int_{\Gamma_1} \hat{u} \frac{\partial w}{\partial n} d\Gamma_1 \tag{2.3}$$

The integral on the left side of Eq. (2.3) is the only term in this equation which is in the domain of the system. In order to obtain a weak form on the boundary of the domain, the nontrivial Laplacian of the weighting function must be computed to sample out the solution from the integral. This is performed using the point collocation method. In point collocation method, the residual of the solution in the domain is set to zero and thus the residual exists only on the boundary of the domain. This condition is satisfied if the weighted residual function is chosen as:

$$\nabla^2 w = -\delta(x-\xi) \tag{2.4}$$

where ξ is the source point or a point at which a concentrated charge such as a concentrated force is acting, x is the field point at which the response of the concentrated charge is considered, and $\delta(x-\xi)$ is the Dirac delta function having the properties:

$$\int_{\Omega} \delta(x) d\Omega = 1 \tag{2.5}$$

$$\int_{\Omega} \delta(x-\xi) f(x) d\Omega = f(\xi) \tag{2.6}$$

The solution to Eq. (2.4) is called the fundamental solution to Laplace equation or the Green's function and is given the symbol u^*. Because of the need for reduction in the dimension of the approximation in the boundary element formulation, only partial differential equations with a known Green's function can be used. In this chapter, Green's function for an isotropic domain for the Laplace equation is known and used in the formulation. However, there is no loss in generality, and the same procedure can be performed for any linear elliptic partial differential equation whose fundamental solution is known. For a two-dimensional isotropic domain the solution to Eq. (2.4) is:

$$u^* = -\frac{1}{2\pi}\ln(r) \tag{2.7}$$

$$q^* = -\frac{1}{2\pi r^2}(x-\xi)\cdot n \tag{2.8}$$

where $r = |x-\xi|$ is the distance between the source point ξ and any point of interest x.

Considering $w = u^*$ and $q^* = \frac{\partial u^*}{\partial n}$ in Eq. (2.3) yields:

$$\int_{\Omega} \nabla^2 u^* u d\Omega = -\int_{\Gamma_2} \hat{q} u^* d\Gamma_2 - \int_{\Gamma_1} q u^* d\Gamma_1 + \int_{\Gamma_2} u q^* d\Gamma_2 + \int_{\Gamma_1} \hat{u} q^* d\Gamma_1 \tag{2.9}$$

By substituting Eq. (2.4) into Eq. (2.9), the solution in the domain integral is sampled out resulting in the integral terms only on the boundary of the system:

$$u(\xi) + \int_{\Gamma_2} uq^* d\Gamma_2 + \int_{\Gamma_1} \hat{u}q^* d\Gamma_1 = \int_{\Gamma_2} \hat{q}u^* d\Gamma_2 + \int_{\Gamma_1} qu^* d\Gamma_1, \quad \xi \in \Omega \tag{2.10}$$

Considering mixed boundary conditions on the boundary Γ, Eq. (2.10) is rewritten as:

$$u(\xi) + \int_{\Gamma} q^*(x,\xi)u(x)dx = \int_{\Gamma} u^*(x,\xi)q(x)dx, \quad \xi \in \Omega \tag{2.11}$$

To obtain all terms in Eq. (2.11) on the boundary of the system, Eq. (2.11) is integrated such that the source point ξ is enclosed by a circular boundary of radius ε as $\varepsilon \to 0$ (Figure 2.1).

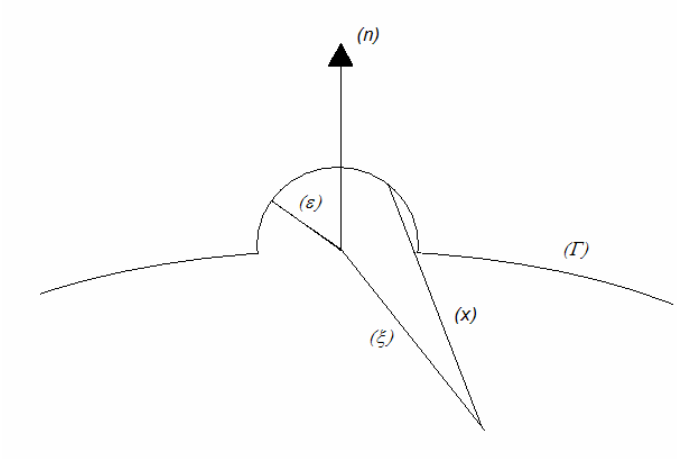

Figure 2.1. Reduction of the dimension of approximation in boundary element formulation.

By substituting Eq. (2.7) into Eq. (2.11), it is shown that the right side integral of Eq. (2.11) vanishes at the limit as $\varepsilon \to 0$:

$$\lim_{\varepsilon \to 0} \int_{\Gamma} -\frac{1}{2\pi} \ln(r) q d\Gamma = \lim_{\varepsilon \to 0} \int_{\theta=0}^{\alpha} -\frac{1}{2\pi} \ln(\varepsilon) q \varepsilon d\theta = -\frac{1}{2\pi} \lim_{\varepsilon \to 0} \int_{\theta=0}^{\alpha} \frac{\ln(\varepsilon) q}{1/\varepsilon} d\theta = 0 \tag{2.12}$$

By substituting Eq. (2.8) into Eq. (2.11), it is shown that the left side integral of Eq. (2.11) results in $-\frac{1}{2}u(\xi)$:

$$\lim_{\varepsilon\to 0}\int_{\Gamma} -\frac{u}{2\pi r^2}(x-\xi)\cdot n d\Gamma = \lim_{\varepsilon\to 0}\int_{\theta=0}^{\alpha} -\frac{u\varepsilon}{2\pi\varepsilon^2}\varepsilon d\theta = -\frac{1}{2\pi}\lim_{\varepsilon\to 0}\int_{\theta=0}^{\alpha} u d\theta = -\frac{\alpha}{2\pi}u \quad (2.13)$$

where α is an angle on the boundary with a value of $\alpha=\pi$ for smooth boundaries. Thus, Eq. (2.11) can be rewritten on the boundary as:

$$\frac{1}{2}u(\xi)+\int_{\Gamma} q^*(x,\xi)u(x)dx = \int_{\Gamma} u^*(x,\xi)q(x)dx,\ \ \xi\in\Gamma \quad (2.14)$$

Equations of the form of Eq. (2.14) are the starting point of the boundary element formulation.

2.2 Constant Boundary Element Discretization

The continuous Eq. (2.14) can be discretized by dividing the continuous boundary Γ into boundary elements Γ_i consisting of nodes at which a value of either u or q is known with assumed polynomial interpolation functions between nodes. For convenience, in this work only boundary elements with constant interpolation functions are used. However, the methodology can be directly extended to higher order approximations. Constant elements contain one node per element, leading to the following approximation:

$$u(x)=\Phi(x)u_i \quad (2.15)$$

$$q(x)=\Phi(x)q_i \quad (2.16)$$

where u_i and q_i are the vectors of nodal values of u and q, respectively, at node i and $\Phi(x)$ is the vector of constant interpolation functions. In general $\Phi(x)$ is the vector of

polynomial interpolation functions between the values of u_i and q_i. The discretized form of Eq. (2.14) can be written in the following form:

$$\frac{1}{2}u_i + \sum_{Elements} \int_{\Gamma} q^*(x,\xi)\Phi(x)dx u_i = \sum_{Elements} \int_{\Gamma} u^*(x,\xi)\Phi(x)dx q_i \tag{2.17}$$

Eq. (2.17) can be written in a matrix form as:

$$Hu = Gq \tag{2.18}$$

where matrix H is singular and matrix G is regular, therefore, the Dirichlet boundary condition must be known on at least one element for the solution to be unique. Eq. (2.18) is rearranged according to the appropriate boundary conditions and solved as a linear algebra problem:

$$Ax = b \tag{2.19}$$

The coefficients of H and G matrices can either be determined explicitly or are computed numerically. Chapter VII describes numerical integration by the use of Taylor series expansion (Taylor 1715); however, other numerical integration schemes can be used following the same methodology.

Chapter III

Boundary Element Analysis in Engineering Mechanics

Chapter III discusses the usage of boundary element method in engineering mechanics. Although boundary element analysis can be performed for skeletal elements, such as truss element and beam element, the use of the skeletal elements is limited due to the discontinuity in the boundary of the system. The boundary element method is more often used for continuum problems such as torsion problem and elasticity problem.

3.1 Torsion Problem

Torsion of circular bars is a well known engineering problem to which a solution can be relatively easily obtained due to the rotational symmetry of the circular cross-section. Due to the rotational symmetry, sections which are in some plane in the un-deformed geometry remain in the same plane in the deformed geometry (Saada 1993). The torsional behavior of noncircular cross-sections is a much harder problem since noncircular cross-sections do not have a rotational symmetry and thus sections which are in some plane in the un-deformed geometry do not remain in the same plane in the deformed geometry. This is a direct result of the shear stress distribution which is nonlinear for an arbitrary cross-section (Shames and Pitarresi 2000). The torsion problem can be expressed in terms of a Laplacian of the warping function ψ, which describes the behavior of the out-of-plane behavior of the cross-section:

$$\nabla^2 \psi = 0 \quad in\ \Omega \tag{3.1}$$

The Laplace equation in Chapter II, Eq. (2.1), consisted of either the Dirichlet or the Neumann boundary conditions which were known on the boundary. However, the torsion problem is a Neumann problem and therefore only the Neumann boundary conditions are known on the boundary of the domain as:

$$\left(\frac{\partial \psi}{\partial x_1} - x_2\right)\frac{dx_2}{ds} - \left(\frac{\partial \psi}{\partial x_2} + x_1\right)\frac{dx_1}{ds} = 0 \quad on\ \Gamma \tag{3.2}$$

For illustrative purpose, a rectangular cross-section with base of $2a$ and height of $2b$ is considered (Figure 3.1).

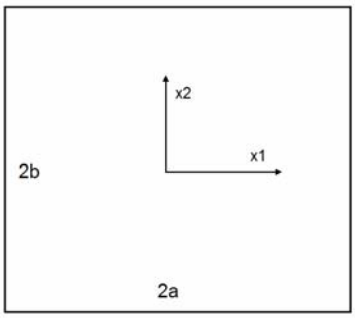

Figure 3.1. Cross-section of a rectangular beam.

The Neumann boundary conditions on the boundary of the above rectangular section are given as:

$$\frac{\partial \psi}{\partial x_1} = \frac{\partial \psi}{\partial n_1}\frac{\partial n_1}{\partial x_1} = x_2, \;\; x_1 = a \tag{3.3}$$

$$\frac{\partial \psi}{\partial x_1} = \frac{\partial \psi}{\partial n_1}\frac{\partial n_1}{\partial x_1} = -x_2, \;\; x_1 = -a \tag{3.4}$$

$$\frac{\partial \psi}{\partial x_2} = \frac{\partial \psi}{\partial n_2}\frac{\partial n_2}{\partial x_2} = -x_1, \;\; x_2 = b \tag{3.5}$$

$$\frac{\partial \psi}{\partial x_2} = \frac{\partial \psi}{\partial n_2}\frac{\partial n_2}{\partial x_2} = x_1, \;\; x_2 = -b \tag{3.6}$$

In order to simplify the boundary conditions, a modified warping function ψ_1 can be introduced. There is no change in the physics of the problem and the warping function substitution is purely made to simplify the computation. The torsion problem can be restated as:

$$\nabla^2 \psi_1 = 0 \quad in\ \Omega \tag{3.7}$$

where ψ_1 is defined as:

$$\psi_1 = x_1 x_2 - \psi \tag{3.8}$$

The Neumann boundary conditions are then expressed as (Figure 3.2):

$$\frac{\partial \psi_1}{\partial x_1} = 0 \quad on\ x_1 = \pm a \tag{3.9}$$

$$\frac{\partial \psi_1}{\partial x_2} = 2x_1 \quad on\ x_2 = b \tag{3.10}$$

$$\frac{\partial \psi_1}{\partial x_2} = -2x_1 \quad on\ x_2 = -b \tag{3.11}$$

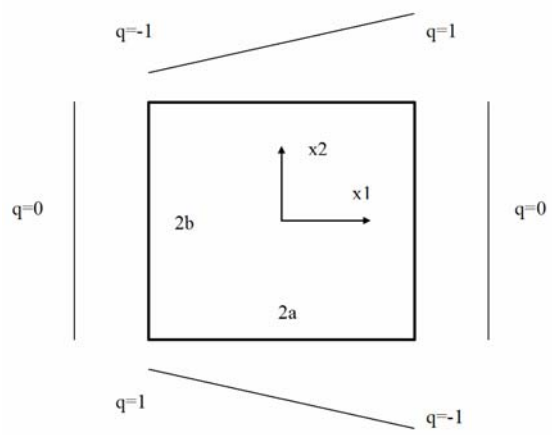

Figure 3.2. Neumann boundary conditions for a torsion problem of a rectangular beam.

The true solution for the torsion of a rectangular bar (Saada 1993) is:

$$\psi_1 = \frac{32a^2}{\pi^3}\sum_{n=0}^{\infty}\frac{(-1)^n \sin(k_n x_1)\sinh(k_n x_2)}{(2n+1)^3 \cosh(k_n b)} \tag{3.12}$$

$$k_n = \frac{(2n+1)\pi}{2a} \tag{3.13}$$

By substituting Eq. (3.12) into Eq. (3.8), the exact solution for the warping function can be obtained:

$$\psi = x_1 x_2 - \frac{32a^2}{\pi^3}\sum_{n=0}^{\infty}\frac{(-1)^n \sin(k_n x_1)\sinh(k_n x_2)}{(2n+1)^3 \cosh(k_n b)} \tag{3.14}$$

In general the exact solution to the torsion problem cannot be found due to the complications in the geometry of the cross-section and the applied Neumann boundary conditions. Numerical methods such as BEM are used to solve for the unknown warping function (Pilkey and Wunderlich 1994). From the approximate solution of the warping function the approximate values of stresses and strains can be computed.

3.2 Boundary Element Analysis of the Torsion Problem

The boundary element formulation for the torsion problem is the same as described in Chapter II. However, the application of boundary conditions deserves a special consideration since only the Neumann boundary conditions are known for the torsion problem. The boundary element formulation requires that at least one element, and therefore a part of the boundary, must have a known Dirichlet boundary condition, which in the case of the torsion problem is the warping function. Since the warping function is unknown prior to solving a problem, a value at which the warping function is zero can be picked arbitrarily. For the rectangular cross-section the warping function ψ_1

is zero at the mid-point of all the sides. In this work, BEA is performed assuming that the exact solution for the warping function is known for one element (Figure 3.3).

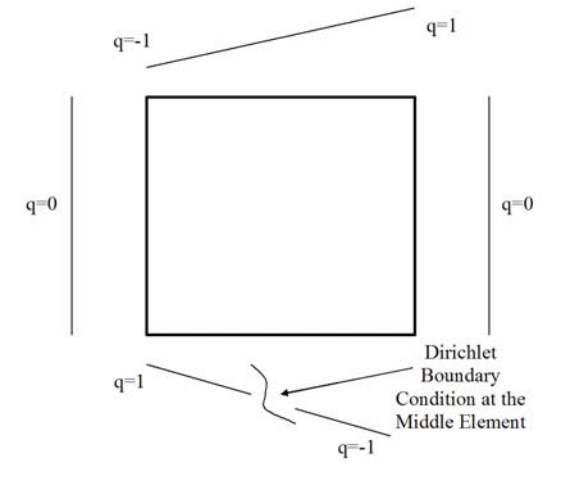

Figure 3.3. Boundary conditions for the boundary element analysis.

Moreover, the applied boundary conditions are considered on the boundary integral equation level, thus, the known boundary conditions are not approximated by polynomial approximations. The Neumann boundary conditions are evaluated explicitly as:

$$\int_{\Gamma} \psi_1^*(x,\xi)\frac{\partial \psi_1}{\partial n}(x)dx, \quad \xi \in \Gamma \tag{3.15}$$

The single Dirichlet boundary condition (Figure 3.3) is evaluated as following:

$$\frac{1}{2}\psi_1(\xi) + \int_{\Gamma} \frac{\partial \psi_1^*}{\partial n}(x,\xi)\psi_1(x)dx, \quad \xi \in \Gamma \tag{3.16}$$

where $\psi_1(\xi)$ is the value of the warping function at the node.

3.3 Boundary Element Formulation for the Elasticity Problem

The boundary element formulation for the behavior of an isotropic and homogeneous body is discussed in literature (Beskos 1989, Brebbia 1978, Brebbia and Dominguez 1992, Hartman 1989, Linkov 2002, Pilkey and Wunderlich 1994). The following section reviews the boundary element formulation for the elasticity problem. The elasticity problem is:

$$\left.\begin{array}{c} \sigma_{ij,j} + b_i = 0 \quad in\ \Omega \\ u_i = \hat{u}_i \quad on\ \Gamma_1 \\ t_i = \hat{t}_i \quad on\ \Gamma_2 \\ \bigcup_{i=1}^{2} \Gamma_i = \Gamma \quad and \quad \bigcap_{i=1}^{2} \Gamma_i = 0 \end{array}\right\} \tag{3.17}$$

where Ω is the domain of the system, Γ is the boundary of the domain, σ_{ij} is the stress tensor, b_i is the vector of body force, u_i is the displacement vector with a Dirichlet boundary condition $\hat{u}_i$ on Γ_1, and t_i is the traction vector with a Neumann boundary condition $\hat{t}_i$ on Γ_2. As for the Laplace problem, the solution to Eq. (3.17) cannot be in general obtained and it must be approximated by numerical techniques. The first step in approximating the solution to Eq. (3.17) is to express it in a weighted residual form or the weak form:

$$\int_{\Omega} \left(\sigma_{ij,j} + b_i\right) u_i^* d\Omega = \int_{\Gamma_2} (t_i - \hat{t}_i) u_i^* d\Gamma_2 - \int_{\Gamma_1} (u_i - \hat{u}_i) t_i^* d\Gamma_1 \tag{3.18}$$

where u_i^* and t_i^* are the vector of weighted residual functions. In the following steps Betti's reciprocal theorem is reviewed and used to formulate boundary integral equations. Considering the weighted equilibrium condition from Eq. (3.18) and expanding results in:

$$\int_{\Omega}\left(\sigma_{ij,j}+b_i\right)u_i^* d\Omega=\int_{\Omega}\sigma_{ij,j}u_i^* d\Omega+\int_{\Omega}b_i u_i^* d\Omega=0 \tag{3.19}$$

Applying the chain rule to the first integral in the right side expansion from Eq. (3.19):

$$\int_{\Omega}\sigma_{ij,j}u_i^* d\Omega=\int_{\Omega}\left(\sigma_{ij}u_i^*\right)_{,j}d\Omega-\int_{\Omega}\sigma_{ij}u_{i,j}^* d\Omega \tag{3.20}$$

Substituting for $u_{i,j}^*=\varepsilon_{ij}^*$ in Eq. (3.20) results in:

$$\int_{\Omega}\sigma_{ij,j}u_i^* d\Omega=\int_{\Omega}\left(\sigma_{ij}u_i^*\right)_{,j}d\Omega-\int_{\Omega}\sigma_{ij}\varepsilon_{ij}^* d\Omega \tag{3.21}$$

where ε_{ij} is the linear strain tensor. Applying Gauss integral theorem to the first integral on the right side in Eq. (3.21):

$$\int_{\Omega}\left(\sigma_{ij}u_i^*\right)_{,j}d\Omega=\int_{\Gamma}\sigma_{ij}u_i^* n_j d\Gamma=\int_{\Gamma}\sigma_{ij}n_j u_i^* d\Gamma=\int_{\Gamma}t_i u_i^* d\Gamma \tag{3.22}$$

Substituting the result of Eq. (3.22) into Eq. (3.21) and rearranging terms yields:

$$\int_{\Omega}\sigma_{ij}\varepsilon_{ij}^* d\Omega+\int_{\Omega}\sigma_{ij,j}u_i^* d\Omega=\int_{\Gamma}t_i u_i^* d\Gamma \tag{3.23}$$

The equilibrium condition, $\sigma_{ij,j}=-b_i$, is substituted into Eq. (3.23) to obtain:

$$\int_{\Omega}\sigma_{ij}\varepsilon_{ij}^* d\Omega-\int_{\Gamma}b_i u_i^* d\Gamma=\int_{\Gamma}t_i u_i^* d\Gamma \tag{3.24}$$

Following the same procedure, Eq. (3.19) through Eq. (3.24), the following equation can be obtained:

$$\int_{\Omega}\sigma_{ij}^*\varepsilon_{ij} d\Omega-\int_{\Gamma}b_i^* u_i d\Gamma=\int_{\Gamma}t_i^* u_i d\Gamma \tag{3.25}$$

It is then considered that the body follows the linear elastic constitutive model:

$$\sigma_{ij}=E_{ijkl}\varepsilon_{kl} \tag{3.26}$$

where E_{ijkl} is the fourth order linear elasticity tensor. Eq. (3.26) can also be written as:

$$\sigma_{ij} = \frac{E}{1+\nu}\varepsilon_{ij} + \frac{\nu E}{(1+\nu)(1-2\nu)}\delta_{ij}\varepsilon_{kk} \tag{3.27}$$

Also by expansion of σ_{ij} tensor and symmetry of E_{ijkl} with respect i, j and k, l indices:

$$\sigma_{ij}\varepsilon_{ij}^{*} = E_{ijkl}\varepsilon_{kl}\varepsilon_{ij}^{*} = E_{klij}\varepsilon_{ij}\varepsilon_{kl}^{*} = E_{klij}\varepsilon_{kl}^{*}\varepsilon_{ij} = E_{ijkl}\varepsilon_{kl}^{*}\varepsilon_{ij} = \sigma_{ij}^{*}\varepsilon_{ij} \tag{3.28}$$

By equating the first integral terms in Eq. (3.24) and Eq. (3.25) due to Eq. (3.28), Betti's reciprocal theorem can be obtained:

$$\int_{\Gamma} t_i u_i^{*} d\Gamma + \int_{\Gamma} b_i u_i^{*} d\Gamma = \int_{\Gamma} t_i^{*} u_i d\Gamma + \int_{\Gamma} b_i^{*} u_i d\Gamma \tag{3.29}$$

Substituting equilibrium equation $\sigma_{ij,j}^{*} = -b_i^{*}$ into Eq. (3.29) and rearranging terms results in:

$$-\int_{\Gamma} \sigma_{ij,j}^{*} u_i d\Gamma + \int_{\Gamma} t_i^{*} u_i d\Gamma = \int_{\Gamma} u_i^{*} b_i d\Gamma + \int_{\Gamma} u_i^{*} t_i d\Gamma \tag{3.30}$$

In order to decrease the dimension of the integral equation, Eq. (3.30), the weighted residual function is set to be the Green's function, which is obtained by applying a point load in direction a_i. This can be written as:

$$\sigma_{ij,j}^{*} = -\delta(x-\xi)a_i \tag{3.31}$$

where ξ is a source point at which a concentrated force is applied, x is a field point at which the response of the system to the application of the concentrated force is observed, and $\delta(x-\xi)$ is the Dirac delta function. The resulting fundamental solution is:

$$u_i^{*} = u_{ji}^{*} a_j \tag{3.32}$$

$$t_i^{*} = t_{ji}^{*} a_j \tag{3.33}$$

where u_{ji}^{*} and t_{ji}^{*} are i components of the displacements and tractions, respectively, due to a concentrated force in the j direction, and a_j is a unit vector in the direction of the applied concentrated force. The kernel functions u_{ji}^{*} and t_{ji}^{*} are given as:

$$u_{ij}^{*} = \frac{1}{8\pi(1-\nu)G}\left[(4\nu-3)\ln(r)\delta_{ij} + \frac{(\vec{x}-\vec{\xi})\bullet\vec{i}}{r}\cdot\frac{(\vec{x}-\vec{\xi})\bullet\vec{j}}{r}\right] \tag{3.34}$$

$$q_{ij}^{*} = \frac{-1}{4\pi(1-\nu)r}\left\{\begin{array}{c}\left[(1-2\nu)\delta_{ij} + 2\dfrac{(\vec{x}-\vec{\xi})\bullet\vec{i}}{r}\cdot\dfrac{(\vec{x}-\vec{\xi})\bullet\vec{j}}{r}\right]\cdot\dfrac{(\vec{x}-\vec{\xi})\bullet\vec{n}}{r} \\ -(1-2\nu)\left[\dfrac{(\vec{x}-\vec{\xi})\bullet\vec{i}}{r}n_y - \dfrac{(\vec{x}-\vec{\xi})\bullet\vec{j}}{r}n_x\right]\end{array}\right\} \tag{3.35}$$

Substituting Eq.(3.31), Eq. (3.32), and Eq. (3.33) into Eq. (3.30) yields:

$$u_i(\xi)a_i + \int_\Gamma t_{ji}^{*}a_j u_i d\Gamma = \int_\Gamma u_{ji}^{*}a_j b_i d\Gamma + \int_\Gamma u_{ji}^{*}a_j t_i d\Gamma, \quad \xi\in\Omega \tag{3.36}$$

The indices are exchanged in all the integral terms in Eq. (3.36) as:

$$u_i(\xi)a_i + \int_\Gamma t_{ij}^{*}a_i u_j d\Gamma = \int_\Gamma u_{ij}^{*}a_i b_j d\Gamma + \int_\Gamma u_{ij}^{*}a_i t_j d\Gamma, \quad \xi\in\Omega \tag{3.37}$$

The a_i coefficients are constant and can be canceled out from Eq. (3.37):

$$u_i(\xi) + \int_\Gamma t_{ij}^{*}u_j d\Gamma = \int_\Gamma u_{ij}^{*}b_j d\Gamma + \int_\Gamma u_{ij}^{*}t_j d\Gamma, \quad \xi\in\Omega \tag{3.38}$$

Assuming that the body force is zero, Eq. (3.38) can be simplified to:

$$u_i(\xi) + \int_\Gamma t_{ij}^{*}u_j d\Gamma = \int_\Gamma u_{ij}^{*}t_j d\Gamma, \quad \xi\in\Omega \tag{3.39}$$

Eq. (3.39) is integrated such that the source point, ξ, is enclosed by the circular boundary of radius ε, as $\varepsilon\to 0$ (Figure 2.1). This results in the right side integral vanishing. For

constant elements the left side integral results in $-\frac{1}{2}u(\xi)$. Thus on the boundary of the system, Eq. (3.39) can be rewritten as:

$$\frac{1}{2}u_i(\xi) + \int_\Gamma t_{ij}^*(x,\xi)u_j(x)dx = \int_\Gamma u_{ij}^*(x,\xi)t_j(x)dx, \quad \xi \in \Gamma \tag{3.40}$$

3.4 Boundary Element Discretization for the Elasticity Problem

In general the boundary integral equation, such as Eq. (3.40), cannot be solved analytically. To obtain approximate solutions, the boundary integral equation is discretized into boundary elements for which the true solution is approximated by a polynomial interpolation between known values of either u or t. In this work, only boundary elements with constant shape functions are used to generate significant discretization errors. Higher order polynomials are assumed to approximate the true solutions better and thus have a smaller discretization error associated with them. Constant elements contain one node per element, leading to the following discretization:

$$u_j(x) = \Phi_{jk}(x)u_k \tag{3.41}$$

$$t_j(x) = \Phi_{jk}(x)t_k \tag{3.42}$$

where u_k and t_k are the vectors of nodal values of $u_j(x)$ or $t_j(x)$, respectively, at node k and $\Phi_{jk}(x)$ is the matrix of constant interpolation functions. The discretized Eq. (3.40) is written as:

$$\frac{1}{2}u_i + \sum_{Elements}\int_\Gamma t_{ij}^*(x,\xi)\Phi_{jk}(x)dx u_k = \sum_{Elements}\int_\Gamma u_{ij}^*(x,\xi)\Phi_{jk}(x)dx t_k \tag{3.43}$$

Eq. (3.43) can be written in a matrix form:

$$Hu = Gt \tag{3.44}$$

where matrix H is singular and therefore the system satisfies the rigid body motion. To obtain a unique solution to Eq. (3.44) at least one boundary condition for the displacement must be specified in each dimension of the problem. Eq. (3.44) is rearranged according to the appropriate boundary conditions and solved as a linear algebra problem:

$$Ax = b \tag{3.45}$$

The coefficients of H and G matrices can either be determined explicitly or are computed numerically. Chapter VII describes numerical integration by the use of Taylor series expansion (Taylor 1715); however, other numerical integration schemes can be used following the same methodology.

Chapter IV

Interval Analysis

Chapter IV reviews some of the interval operations which are used throughout the latter chapters.

4.1 Interval Operations

Interval mathematics is described in literature (Alefeld and Herzberger 1983, Moore 1966, Neumaier 1990). The following chapter is a summary of the interval operations. An interval number $\tilde{x} = [a, b]$ is a set of real numbers such that:

$$[a, b] = \{x \mid a \leq x \leq b\} \tag{4.1}$$

where $(a, b) \in \Re$. Two interval numbers $\tilde{x} = [a, b]$ and $\tilde{y} = [c, d]$ behave according to the following operations:

Addition:

$$\tilde{x} + \tilde{y} = [a + c, b + d] \tag{4.2}$$

Subtraction:

$$\tilde{x} - \tilde{y} = [a - d, b - c] \tag{4.3}$$

Multiplication:

$$\tilde{x} \cdot \tilde{y} = [\min(ac, ad, bc, bd), \max(ac, ad, bc, bd)] \tag{4.4}$$

Division:

$$\frac{\tilde{x}}{\tilde{y}} = [a, b] \cdot \left[\frac{1}{d}, \frac{1}{c}\right] \quad , \quad 0 \notin \tilde{y} \tag{4.5}$$

Enclosure:

$$\tilde{x} \supset \tilde{y} \Rightarrow a < c < d < b \tag{4.6}$$

$$\tilde{x} \supseteq \tilde{y} \Rightarrow a \le c \le d \le b \tag{4.7}$$

Associative property:

$$\tilde{x} + (\tilde{y} + \tilde{z}) = (\tilde{x} + \tilde{y}) + \tilde{z} \tag{4.8}$$

$$\tilde{x} \cdot (\tilde{y} \cdot \tilde{z}) = (\tilde{x} \cdot \tilde{y}) \cdot \tilde{z} \tag{4.9}$$

Commutative property:

$$\tilde{x} + \tilde{y} = \tilde{y} + \tilde{x} \tag{4.10}$$

$$\tilde{x} \cdot \tilde{y} = \tilde{y} \cdot \tilde{x} \tag{4.11}$$

Subdistributivity property:

$$\tilde{x} \cdot (\tilde{y} + \tilde{z}) \subseteq \tilde{x} \cdot \tilde{y} + \tilde{x} \cdot \tilde{z} \tag{4.12}$$

If $\tilde{y} \cdot \tilde{z} > 0$:

$$\tilde{x} \cdot (\tilde{y} + \tilde{z}) = \tilde{x} \cdot \tilde{y} + \tilde{x} \cdot \tilde{z} \tag{4.13}$$

If $x \in \Re$, for any $\tilde{y}$ and $\tilde{z}$:

$$x \cdot (\tilde{y} + \tilde{z}) = x \cdot \tilde{y} + x \cdot \tilde{z} \tag{4.14}$$

The interval numbers exhibit identities with respect to 0 and 1 in interval addition and interval multiplication, respectively:

$$0 + \tilde{x} = \tilde{x} + 0 = \tilde{x} \tag{4.15}$$

$$1 \cdot \tilde{x} = \tilde{x} \cdot 1 = \tilde{x} \tag{4.16}$$

One of the most interesting behaviors of interval numbers is the interval dependency. For an interval number $\tilde{x} = [a, b]$ and an interval number $\tilde{y} = [a, b]$

multiplying $\tilde{x} \cdot \tilde{x}$ and $\tilde{x} \cdot \tilde{y}$ results in different bounds if $a < 0$, $b > 0$. In the first multiplication every number within the set $\tilde{x}$ has to be multiplied by itself. This is not true for the second multiplication since it is assumed that the two sets $\tilde{x}$ and $\tilde{y}$ are independent sets. The resulting bounds are:

$$\tilde{x} \cdot \tilde{x} = \left[0, \max\left(a^2, b^2\right)\right] \tag{4.17}$$

$$\tilde{x} \cdot \tilde{y} = [ab, \max(a^2, b^2)] \tag{4.18}$$

Interval dependency must be considered in the calculations to obtain sharp and realistic results. For matrices with interval coefficients, the interval operations should be performed at the last stage to obtain sharp results. This procedure allows preserving interval dependency. The following example illustrates this consideration. Let there be two interval vectors $\tilde{y}_1 = A \cdot (B \cdot \tilde{x}),\ \tilde{y}_2 = (A \cdot B) \cdot \tilde{x}$ where:

$A = \begin{bmatrix} \mathrm{a}_{11} & a_{12} \\ a_{21} & a_{22} \end{bmatrix},\ B = \begin{bmatrix} b_{11} & b_{12} \\ b_{21} & b_{22} \end{bmatrix},\ \tilde{x} = \begin{bmatrix} \tilde{x}_1 \\ \tilde{x}_2 \end{bmatrix}$. It is clear that the two vectors are formed by the same matrices and vector, however, because of the order of operations they differ. Computing the two vectors:

$$\tilde{y}_1 = \begin{bmatrix} a_{11}(b_{11}\tilde{x}_1 + b_{12}\tilde{x}_2) + a_{12}(b_{21}\tilde{x}_1 + b_{22}\tilde{x}_2) \\ a_{21}(b_{11}\tilde{x}_1 + b_{12}\tilde{x}_2) + a_{22}(b_{21}\tilde{x}_1 + b_{22}\tilde{x}_2) \end{bmatrix},\ \tilde{y}_2 = \begin{bmatrix} (a_{11}b_{11} + a_{12}b_{21})\tilde{x}_1 + (a_{11}b_{12} + a_{12}b_{22})\tilde{x}_2 \\ (a_{21}b_{11} + a_{22}b_{21})\tilde{x}_1 + (a_{21}b_{12} + a_{22}b_{22})\tilde{x}_2 \end{bmatrix}$$

it can be clearly seen that $\tilde{y}_2$ is sharper then $\tilde{y}_1$ due to considered dependency of $\tilde{x}_1$ and $\tilde{x}_2$ throughout the rows of $\tilde{y}_2$. Special care should be given to the order of interval operations to obtain sharp bounds on the solution.

4.2 Interval Enclosure

The following section describes the enclosure of interval sets. The enclosure has to be guaranteed for the interval solution to interval linear system of equations and is used in the latter interval solvers. Monotonic inclusion for sets $\tilde{x}$ and $\tilde{y}$ where $\tilde{x} \subset \tilde{w}$ and $\tilde{y} \subset \tilde{z}$ is:

$$\tilde{x} + \tilde{y} \subset \tilde{w} + \tilde{z} \tag{4.19}$$

$$\tilde{x} - \tilde{y} \subset \tilde{w} - \tilde{z} \tag{4.20}$$

$$\tilde{x} \cdot \tilde{y} \subset \tilde{w} \cdot \tilde{z} \tag{4.21}$$

$$\frac{\tilde{x}}{\tilde{y}} \subset \frac{\tilde{w}}{\tilde{z}},\ 0 \notin \tilde{y},\ 0 \notin \tilde{z} \tag{4.22}$$

The integral of an interval valued function $f(\tilde{x})$, which is the class of all possible functions bounded by a given interval, such that $f(x) \in [\underline{f}(x), \overline{f}(x)]$, is performed as:

$$\int_x f(\tilde{z})dz = [\int_x \underline{f}(z)dz, \int_x \overline{f}(z)dz] \tag{4.23}$$

If $f(\tilde{x}) \subset g(\tilde{x})$ then:

$$\int_x f(\tilde{z})dz \subset \int_x g(\tilde{z})dz \tag{4.24}$$

4.3 Krawczyk Iteration for Interval Linear System of Equations

The majority of interval systems are solved using iterative techniques. The following two sections describe the iterative methods for solving interval linear system of equations. The interval linear system of equations can be written as:

$$\tilde{A}\tilde{x} = \tilde{b} \tag{4.25}$$

The solution to these kinds of problems has been studied since 1965 (Hansen 1965). In this work two iterative methods are considered, Krawczyk iteration (Krawczyk 1969, Neumaier 1990) and interval Gauss-Seidel iteration (Neumaier 1990). The interval linear system of equations Eq. (4.25) is solved using Krawczyk iteration based on Brouwer's fixed point theorem (Mullen and Muhanna 1999, Muhanna and Mullen 2001, Muhanna et al. 2005). One approach of self-validating (SV) methods to find the zero of the function $f(x) = 0,\ \Re^n \to \Re^n$ is to consider a fixed point function $g(x) = x$. The transformation between $f(x)$ and $g(x)$ for a non-singular preconditioning matrix C is:

$$f(x) = 0 \Leftrightarrow g(x) = x \tag{4.26}$$

$$g(x) = x - C \cdot f(x) \tag{4.27}$$

where the function $g(x)$ is considered as a Newton operator. From Brouwer's fixed point theorem and from:

$$g(\tilde{x}) \subseteq \tilde{x} \quad for\ some\ \tilde{x} \in \Re^n \tag{4.28}$$

the following is true:

$$\exists\ x \in \tilde{x}: \quad f(x) = 0 \tag{4.29}$$

This method is used to solve linear system of equations, Eq. (4.25). The preconditioning matrix C is chosen as $C = A^{-1}$. From Eq. (4.27) and Eq. (4.28) it follows that:

$$Cb + (I - CA)\tilde{x} \subseteq \tilde{x} \tag{4.30}$$

The left hand side of Eq. (4.30) is the Krawczyk operator (Krawczyk 1969). For the iteration to provide finite solution, the preconditioning matrix needs to be proven regular (Neumaier 1990, Rump 2001). The following proves this condition.

Theorem 1. (Rump 2001) *Let* $A, C \in \Re^{n \times n}, \tilde{b} \in \Re^n,$ *and* $\tilde{x} \in \Re^n$ *be given*. If

$$Cb + (I - CA)\tilde{x} \subseteq \tilde{x} \tag{4.31}$$

then C and A are regular and the unique solution of $Ax = b$ *satisfies* $A^{-1}b \in \tilde{x}$

$\text{int}(\tilde{x})$ refers to the interior of $\tilde{x}$. However, all terms in Eq. (4.25) are interval terms, thus the following is a proof for the guarantee of the solution for the equation of this form.

Theorem 2. (Rump 2001) *Let* $\tilde{A} \in \Re^{n\times n}, C \in \Re^{n\times n}, \tilde{b} \in \Re^{n}$, *and* $\tilde{x} \in \Re^{n}$ *be given*. If

$$C\tilde{b} + (I - C\tilde{A})\tilde{x} \subseteq \text{int}(\tilde{x}) \tag{4.32}$$

then C and every matrix $A \in \tilde{A}$ *is regular and*

$$\sum(\tilde{A}, \tilde{b}) = \{x \in \Re^{n} \mid \exists\ A \in \tilde{A}\ \exists\ b \in \tilde{b} : Ax = b\} \subseteq \tilde{x} \tag{4.33}$$

Eq. (4.33) guarantees the solution to the interval linear system of equations, Eq. (4.25). The residual form of Eq. (4.33) is (Neumaier 1990):

$$C\tilde{b} - C\tilde{A}x_0 + (I - C\tilde{A})\tilde{\delta} \subseteq \text{int}(\tilde{\delta}) \tag{4.34}$$

where $\tilde{x} = x_0 + \tilde{\delta}$. A good initial guess is $x_0 = C\hat{b}$, where $C = \hat{A}^{-1}$, $\hat{A}$ is the midpoint matrix of A, and $\hat{b}$ is the midpoint vector of b. The Krawczyk iteration can be derived by considering an interval linear system of equations:

$$\tilde{A}_e\tilde{x}_e = \tilde{b}_e \tag{4.35}$$

where $\tilde{A}_e \in \tilde{A}$, $\tilde{b}_e \in \tilde{b}$ and $\tilde{x}_e \in \tilde{x}$. The exact solution can be obtained as:

$$\tilde{x}_e = \tilde{A}_e^{-1}\tilde{b}_e \tag{4.36}$$

Adding zero to the left side and collecting terms results in the following:

$$\tilde{x}_e = \tilde{A}_e^{-1}\tilde{b}_e = C\tilde{b}_e - C\tilde{A}_e\tilde{A}_e^{-1}\tilde{b}_e + \tilde{A}_e^{-1}\tilde{b}_e = C\tilde{b}_e - \left(C\tilde{A}_e - I\right)\left(\tilde{A}_e^{-1}\tilde{b}_e\right) \tag{4.37}$$

Thus:

$$\tilde{A}_e^{-1}\tilde{b}_e \in C\tilde{b} - \left(C\tilde{A} - I\right)\tilde{x}_e \tag{4.38}$$

The hull inverse of a matrix is defined in terms of mapping as:

$$\tilde{A}^H\tilde{b} = \left\{\tilde{A}_e^{-1}\tilde{b}_e \middle| \tilde{A}_e \in \tilde{A}, \tilde{b}_e \in \tilde{b}\right\} \tag{4.39}$$

Eq. (4.38) is rewritten:

$$\tilde{A}^H\tilde{b} \subseteq C\tilde{b} - \left(C\tilde{A} - I\right)\tilde{x}_e \tag{4.40}$$

or:

$$\tilde{A}^H\tilde{b} \subseteq \left[C\tilde{b} - \left(C\tilde{A} - I\right)\tilde{x}\right] \cap \tilde{x} \tag{4.41}$$

The Krawczyk iteration follows as:

$$\tilde{x}_{i+1} \subseteq \left[C\tilde{b} + \left(I - C\tilde{A}\right)\tilde{x}_i\right] \cap \tilde{x}_i \tag{4.42}$$

The convergence of Krawczyk iteration has been improved by ε-inflation (Rump 1980, Rump 1992). For a set $\tilde{x}$ the ε-inflation is defined as:

$$\tilde{x} \circ \varepsilon =: \tilde{x} + U_\varepsilon(0) \tag{4.43}$$

where $U_\varepsilon(0)$ is a closed set or radius ε around the origin of set $\tilde{x}$. Using ε-inflation the iteration is modified as:

$$\tilde{x}_{i+1} \subseteq \left[C\tilde{b} + \left(I - C\tilde{A}\right)\tilde{x}_i \cdot U_\varepsilon(0)\right] \cap \tilde{x}_i \cdot U_\varepsilon(0) \tag{4.44}$$

The residual Krawczyk iteration can be derived as following. First a residual is defined as:

$$\tilde{\delta}_e = \tilde{A}_e^{-1}\tilde{b}_e - \tilde{x}_e \tag{4.45}$$

Adding zero to the residual and collecting terms results in:

$$\tilde{\delta}_e = \tilde{\delta}_e + \left[\left(\tilde{b}_e - \tilde{A}_e\tilde{x}_e\right) - \tilde{A}_e\left(\tilde{A}_e^{-1}\tilde{b}_e - \tilde{x}_e\right)\right] = \tilde{\delta}_e + \left[\left(\tilde{b}_e - \tilde{A}_e\tilde{x}_e\right) - \tilde{A}_e\tilde{\delta}_e\right] \tag{4.46}$$

Multiplying the zero term be a preconditioning matrix C:

$$\tilde{\delta}_e = \tilde{\delta}_e + C\left[\left(\tilde{b}_e - \tilde{A}_e\tilde{x}_e\right) - \tilde{A}_e\tilde{\delta}_e\right] \tag{4.47}$$

Distributing matrix C and collecting terms:

$$\tilde{\delta}_e = \tilde{\delta}_e + C\left(\tilde{b}_e - \tilde{A}_e\tilde{x}_e\right) - C\tilde{A}_e\tilde{\delta}_e = C\left(\tilde{b}_e - \tilde{A}_e\tilde{x}_e\right) + \left(I - C\tilde{A}_e\right)\tilde{\delta}_e \tag{4.48}$$

The iteration follows as:

$$\tilde{\delta}_{i+1} \subseteq \left[C\left(\tilde{b} - \tilde{A}\tilde{x}\right) + \left(I - C\tilde{A}\right)\tilde{\delta}_i\right] \cap \tilde{\delta}_i \tag{4.49}$$

and is terminated when the i^{th} residual encloses the $(i+1)^{\text{th}}$ residual. The iteration using ε-inflation is modified as:

$$\tilde{\delta}_{i+1} \subseteq \left[C\left(\tilde{b} - \tilde{A}\tilde{x}\right) + \left(I - C\tilde{A}\right)\tilde{\delta}_i \cdot U_\varepsilon(0)\right] \cap \tilde{\delta}_i \cdot U_\varepsilon(0) \tag{4.50}$$

4.4 Interval Gauss-Seidel Iteration for Interval Linear System of Equations

A dual method for obtaining solutions to Eq. (4.25) is the interval Gauss-Seidel iteration (Neumaier 1990). This method is based on writing Eq. (4.35) explicitly as:

$$\sum_{j=1}^{n} \tilde{A}_{eij}\tilde{x}_{ej} = \tilde{b}_{ei} \tag{4.51}$$

It is also assumed that $0 \notin \tilde{A}_{eii}$. Solving for the i^{th} unknown in the i^{th} equation results in:

$$\tilde{x}_{ei} = \frac{\tilde{b}_{ei} - \sum_{j=1,\ j\neq i}^{n} \tilde{A}_{eij}\tilde{x}_{ej}}{\tilde{A}_{eii}} \tag{4.52}$$

Also:

$$\tilde{x}_{ei} \subseteq \frac{\tilde{b}_i - \sum_{j=1,\ j\neq i}^{n} \tilde{A}_{ij}\tilde{x}_j}{\tilde{A}_{ii}} \tag{4.53}$$

However, not all the available information coming from iterative solutions has been used in Eq. (4.53). Except for the solution for the first variable in the first iteration, the next iteration can be updated with newly computed solutions. Thus if $\tilde{y}$ is the solution at the $i+1^{\text{th}}$ iterate and $\tilde{x}$ is the solution at the i^{th} iterate, Eq. (4.53) can be rewritten as:

$$\tilde{y}_{ei} \subseteq \frac{\tilde{b}_i - \sum_{j=1,\ j<i}^{n} \tilde{A}_{ij}\tilde{y}_j - \sum_{j=1,\ j>i}^{n} \tilde{A}_{ij}\tilde{x}_j}{\tilde{A}_{ii}} \tag{4.54}$$

The total solution is then found as:

$$\tilde{y} \subseteq \left[\frac{\tilde{b}_i - \sum_{j=1,\ j<i}^{n} \tilde{A}_{ij}\tilde{y}_j - \sum_{j=1,\ j>i}^{n} \tilde{A}_{ij}\tilde{x}_j}{\tilde{A}_{ii}} \right] \bigcap \tilde{x} \tag{4.55}$$

with the stopping criteria being the same as for Krawczyk iteration. Preconditioning Gauss-Seidel iteration further improves the results.

Theorem 3. (Neumaier 1990) *Let* $\tilde{A} \in \Re^{n\times n}, C \in \Re^{n\times n}, \tilde{b} \in \Re^{n}$, *and* $\tilde{x} \in \Re^{n}$ *be given*. If

$$C\tilde{A} = A + \tilde{E} \tag{4.56}$$

then the Krawczyk iterates contain the preconditioned Gauss – Seidel iterates

A good preconditioning matrix C for Eq. (4.25) is A, a midpoint matrix of $\tilde{A}$.

Chapter V

Algorithms for Solving Interval Linear Systems of Equations

Chapter V describes the developed iterative solutions to interval linear systems of equations. All of the iterative schemes described below are based on Krawczyk iteration and thus guarantee the enclosure of the true solution. Those iterative schemes are used to solve the interval linear systems of equations which result from the error analyses described in the latter chapters.

5.1 Sharp Algorithm for Interval Linear System of Equations Using Krawczyk Iteration

The following section presents a developed sharp interval solver used to compute the guaranteed enclosure for the solution to Eq. (4.25). The algorithm gives sharper results than the inbuilt MATLAB 6.5.1, toolbox b4m, algorithm. The initial deterministic guess is first computed as:

$$x_0 = A^{-1}b \tag{5.1}$$

where A^{-1} and b are midpoint matrices of $\tilde{A}$ and $\tilde{b}$ respectively. Then, the difference between I and the preconditioning matrix A^{-1} post-multiplied by the interval matrix $\tilde{A}$ is computed:

$$\tilde{I}_d = I - A^{-1}\tilde{A} \tag{5.2}$$

The difference between the solution and the initial guess is computed and pre-multiplied by the preconditioning matrix A^{-1}:

$$\tilde{\delta} = A^{-1}\left(\tilde{b} - \tilde{A}x_0\right) \tag{5.3}$$

Also:

$$\tilde{\delta}_1 = \tilde{\delta} \tag{5.4}$$

The iteration then follows as:

$$\tilde{del} = \tilde{\delta}_1 \tag{5.5}$$

$$\tilde{\delta}_1 = \tilde{\delta} + \tilde{I}_d \tilde{del} \tag{5.6}$$

$$\text{if } \tilde{\delta}_1 \supset \tilde{del} \text{ return to Eq. (5.5)} \tag{5.7}$$

$$\text{if } \tilde{del} \supset \tilde{\delta}_1 \tag{5.8}$$

$$\tilde{x} = x_0 + \tilde{\delta}_1 \tag{5.9}$$

5.2 Sharp Algorithm for Interval Linear System of Equations Using Krawczyk Iteration and Variable Epsilon Inflation

The enclosure of the true solution to Eq. (4.25), for large widths of interval coefficients of matrix $\tilde{A}$, is generally very wide and consist of large overestimation of the true solution. This is due much to the fact that each iterate is based on the previous iterate and therefore the size of each computed set is directly related to the previously computed set. Thus, the final enclosure depends on the path of iteration which in most cases largely overestimates the true solution. To account for the width of each iterate an algorithm is developed in which the ε-inflation (Rump 1980, Rump 1992) is allowed to vary. Many enclosures are found, using different ε-inflations for each solution, and the sharpest solution is found to be the final enclosure. The only change in the algorithm from the previous section thus occurs at the iteration step in Eq. (5.5):

$$\tilde{d}el = \tilde{\delta}_1 + U_{\varepsilon}(0) \tag{5.10}$$

5.3 Sharp Algorithm for Parametric Interval Linear System of Equations

The previously developed algorithms are incapable of computing sharp or nearly sharp bounds on the solution if the interval linear system of equations is functionally dependent. The above solver considers all matrix and vector coefficients to be independent interval numbers. However, in some cases the entire linear system of equations can be expressed as a function of one variable. In general this function may be complicated and the interval variable cannot be factored out of the system directly. This section describes a developed algorithm to incorporate a single interval dependency into the interval solver from the previous section. Let us assume that the entire system of interval linear equations depend on a single variable $\tilde{\xi}$. The coefficients of the $\tilde{A}$ and $\tilde{b}$ matrices are computed for each subinterval $\tilde{\xi}_i$ such that

$$\bigcup_{i=1}^{n} \tilde{\xi}_i = \tilde{\xi} \;\; and \;\; \bigcap_{i=1}^{n} \tilde{\xi}_i = \tilde{0} \tag{5.11}$$

which results in the interval linear system of equations for each $\tilde{\xi}_i$:

$$\tilde{A}(\tilde{\xi}_i)\tilde{x} = \tilde{b}(\tilde{\xi}_i) \tag{5.12}$$

The initial solution is considered as deterministic and found as:

$$x_0 = A^{-1}b \tag{5.13}$$

where, A and b are the midpoint matrices of $\tilde{A}$ and $\tilde{b}$, respectively. For each subinterval $\tilde{\xi}_i$ a preconditioning matrix is computed:

$$C(\tilde{\xi}_i) = mid\left[\tilde{A}(\tilde{\xi}_i)\right]^{-1} \tag{5.14}$$

The difference between the preconditioning matrix $C(\tilde{\xi}_i)$ post-multiplied by the interval matrix $\tilde{A}(\tilde{\xi}_i)$ and I is computed for every $\tilde{\xi}_i$.

$$\tilde{I}_d(\tilde{\xi}_i) = I - C(\tilde{\xi}_i)\tilde{A}(\tilde{\xi}_i) \tag{5.15}$$

The difference between the solution and the initial guess is computed for each $\tilde{\xi}_i$ and pre-multiplied by the preconditioning matrix $C(\tilde{\xi}_i)$:

$$\tilde{\delta} = \bigcup_{i=1}^{n} C(\tilde{\xi}_i)\left(\tilde{b}(\tilde{\xi}_i) - \tilde{A}(\tilde{\xi}_i)x_0\right) \tag{5.16}$$

Also:

$$\tilde{\delta}_1 = \tilde{\delta} \tag{5.17}$$

The iteration then follows as:

$$\tilde{del} = \tilde{\delta}_1 \tag{5.18}$$

$$\tilde{\delta}_1(\tilde{\xi}_i) = C(\tilde{\xi}_i)\left(\tilde{b}(\tilde{\xi}_i) - \tilde{A}(\tilde{\xi}_i)x_0\right) + \tilde{I}_d(\tilde{\xi}_i)\tilde{del} \tag{5.19}$$

$$\tilde{\delta}_1 = \bigcup_{i=1}^{n} \tilde{\delta}_1(\tilde{\xi}_i) \tag{5.20}$$

$$\text{if } \tilde{\delta}_1 \supset \tilde{del} \text{ return to Eq. (5.18)} \tag{5.21}$$

$$\text{if } \tilde{del} \supset \tilde{\delta}_1 \tag{5.22}$$

$$\tilde{x} = x_0 + \tilde{\delta}_1 \tag{5.23}$$

5.4 Generalized Interval Linear System of Equations

5.4.1 Transformation of Generalized Interval Linear System of Equations to Interval Linear System of Equations

A generalized interval linear system of equations can be written as:

$$\tilde{A}_1\tilde{x} + \tilde{A}_2\tilde{x} = \tilde{b}_1 \tag{5.24}$$

The solution to Eq. (5.24) is not necessarily the same as for Eq. (4.25) due to the subdistributivity property of interval numbers. The solution to Eq. (4.25) can be in fact a subset of the solution to Eq. (5.24) as:

$$\left(\tilde{A}_1 + \tilde{A}_2\right)\tilde{x} = \tilde{A}\tilde{x} \subseteq \tilde{A}_1\tilde{x} + \tilde{A}_2\tilde{x} = \tilde{b}_1 \tag{5.25}$$

This section describes the developed transformation of Eq. (5.24) to be in the form of Eq. (4.25) such that the iterative methods described in the previous sections can be applied. Considering an equation:

$$\tilde{A}_{1e}\tilde{x}_e + \tilde{A}_{2e}\tilde{x}_e = \tilde{b}_{1e} \tag{5.26}$$

where $\tilde{A}_{1e} \in \tilde{A}_1$, $\tilde{A}_{2e} \in \tilde{A}_2$, $\tilde{b}_{1e} \in \tilde{b}_1$, $\tilde{x}_e \in \tilde{x}$ and A_{1e} is regular $\forall A_{1e} \middle| A_{1e} \in \tilde{A}_{1e}$. Pre-multiplying Eq. (5.26) by $\tilde{A}_{1e}^{-1}$ results in:

$$\tilde{A}_{1e}^{-1}\tilde{A}_{1e}\tilde{x}_e + \tilde{A}_{1e}^{-1}\tilde{A}_{2e}\tilde{x}_e = \tilde{A}_{1e}^{-1}\tilde{b}_{1e} \tag{5.27}$$

Letting $\tilde{A}_{1e}^{-1}\tilde{A}_{1e} = I$, $\tilde{A}_{1e}^{-1}\tilde{A}_{2e} = \tilde{A}_{3e}$ and $\tilde{A}_{1e}^{-1}\tilde{b}_{1e} = \tilde{b}_e$, Eq. (5.27) can be written as:

$$\tilde{x}_e + \tilde{A}_{3e}\tilde{x}_e = \tilde{b}_e \tag{5.28}$$

Since the first term in Eq. (5.28) is a deterministic identity matrix pre-multiplying $\tilde{x}_e$, the following substitution can be made directly. Letting $I + \tilde{A}_{3e} = \tilde{A}_e$ results in:

$$\tilde{A}_e \tilde{x}_e = \tilde{b}_e \tag{5.29}$$

Eq. (5.29) is in the form of Eq. (4.25) and thus the iterative methods described previously can be used to obtain its guaranteed solution.

5.4.2 Solver for the Generalized Interval Linear System of Equations

The following section describes a developed algorithm to compute the solution to Eq. (5.24) using Krawczyk iteration. Considering an interval linear system of equations:

$$\tilde{A}_1 \tilde{x} + \tilde{A}_2 \tilde{x} = \tilde{b}_1 \tag{5.30}$$

The system is preconditioned by A_1^{-1}, where A_1 is the midpoint matrix of $\tilde{A}_1$, as:

$$A_1^{-1}\tilde{A}_1 \tilde{x} + A_1^{-1}\tilde{A}_2 \tilde{x} = A_1^{-1}\tilde{b}_1 \tag{5.31}$$

The following substitution is performed $A_1^{-1}\tilde{A}_1 = \tilde{I}_1$, $A_1^{-1}\tilde{A}_2 = \tilde{A}_3$ and $A_1^{-1}\tilde{b}_1 = \tilde{b}$:

$$\tilde{I}_1 \tilde{x} + \tilde{A}_3 \tilde{x} = \tilde{b} \tag{5.32}$$

$\tilde{I}_1$ is replaced by I resulting in:

$$I\tilde{x} + \tilde{A}_3 \tilde{x} = \tilde{b} \tag{5.33}$$

Since I is deterministic it can be directly added to $\tilde{A}_3$. Substituting $I + \tilde{A}_3 = \tilde{A}$ Eq. (5.33) is written as:

$$\tilde{A}\tilde{x} = \tilde{b} \tag{5.34}$$

The iteration proceeds as in the case of solving Eq. (5.34) by the described algorithm. The only difference is the replacement of Eq. (5.3) by:

$$\tilde{\delta} = A^{-1}A_1^{-1}\left(\tilde{b}_1 - \tilde{A}_1 u_0 - \tilde{A}_2 u_0\right) \tag{5.35}$$

5.4.3 Parameterized Solver for the Generalized Interval Linear System of Equations

The previously developed algorithm is incapable of computing sharp or nearly sharp bounds on the solution if the interval linear system of equations is functionally dependent. This section describes a developed algorithm to incorporate a single interval dependency into the interval solver from the previous section. Again, let us assume that the entire system of interval linear equations depend on a single variable $\tilde{\xi}$. The coefficients of the $\tilde{A}_1$, $\tilde{A}_2$, and $\tilde{b}_1$ matrices are computed for each subinterval $\tilde{\xi}_i$ such that Eq. (5.11) holds. The parameterization results in the interval linear system of equations for each $\tilde{\xi}_i$:

$$\tilde{A}_1(\tilde{\xi}_i)\tilde{x} + \tilde{A}_2(\tilde{\xi}_i)\tilde{x} = \tilde{b}_1(\tilde{\xi}_i) \tag{5.36}$$

Preconditioning and substitution as described in the previous section lead to:

$$\tilde{A}(\tilde{\xi}_i)\tilde{x} = \tilde{b}(\tilde{\xi}_i) \tag{5.37}$$

The iteration proceeds as in the case of solving Eq. (5.12) by the described algorithm. Eq. (5.16) is replaced by:

$$\tilde{\delta} = \bigcup_{i=1}^{n} C(\tilde{\xi}_i)A_1^{-1}(\tilde{\xi}_i)\left(\tilde{b}_1(\tilde{\xi}_i) - \tilde{A}_1(\tilde{\xi}_i)x_0 - \tilde{A}_2(\tilde{\xi}_i)x_0\right) \tag{5.38}$$

and Eq. (5.19) is replaced by:

$$\tilde{\delta}_1(\tilde{\xi}_i) = C(\tilde{\xi}_i)A_1^{-1}(\tilde{\xi}_i)\left(\tilde{b}_1(\tilde{\xi}_i) - \tilde{A}_1(\tilde{\xi}_i)x_0 - \tilde{A}_2(\tilde{\xi}_i)x_0\right) + \tilde{I}_d(\tilde{\xi}_i)\tilde{del} \tag{5.39}$$

Chapter VI

Uncertainty in Boundary Conditions

Chapter VI describes the treatment of the uncertain boundary conditions using an interval approach. A computational scheme which obtains exact solutions is also developed.

6.1 Interval Treatment of Uncertainty Present in Boundary Conditions

In already existing engineering systems the boundary conditions, natural or forced, cannot be precisely known due to limitations in the precision of the measurements. However, most engineering systems which are analyzed are not in existence and the boundary conditions must be assumed. Moreover, the engineer has to predict the worst case behavior of the system with the limited resources available. One of the limitations is the knowledge of the boundary conditions that the system is subjected to. Most boundary conditions are determined either from experience, historical data, or from assumption and are not reliable. Due to this uncertainty, for most engineering systems the worst case behavior of the system cannot be determined. For engineering systems with relatively small amount of degrees of freedom, the exact behavior of the system considering bounded uncertainty in boundary conditions can be computed from combinatorial methods. Probabilistic approach can also be used through Monte Carlo simulation (Hammersley and Handscomb 1964) to obtain inner bounds of the true solution to the behavior of the engineering system. This approach, however, does not

guarantee the worst case behavior as only the inner bounds are obtained. Moreover, both the combinatorial and the probabilistic approaches are computationally very expensive and cannot be performed for realistic engineering systems. Despite these limitations in the analysis, an engineer is expected to predict the worst case behavior of the system and to achieve a reliable design.

In this work, the uncertainty in boundary conditions is considered as an interval number resulting in interval vectors $\tilde{u}$ and $\tilde{q}$ (Zalewski et al. 2006). The interval bounds on $\tilde{u}$ and $\tilde{q}$ result from considering an unknown but bounded probability density function. The bounds for an unknown probability density function may come from the lowest and highest observed values from historical data, experimental data, or design criterion. The correct determination of these bounds is not a focus of this work and is to be treated as a separate issue. The interval approach allows to consider all the possible patterns of uncertain boundary conditions and thus to obtain the worst case bounds on the solution. Since interval numbers consider all possible values, interval operations directly give enclosure of the true solution without the large computational expense of performing combinatorial or Monte Carlo simulations. In the consideration of uncertain boundary conditions, the numerical errors are not accounted for and it is assumed that the H and G matrices are computed explicitly. This leads to the interval boundary element method (IBEM) formulation considering the uncertainty in the boundary conditions and the linear system of equations becomes:

$$H\tilde{u} = G\tilde{q} \tag{6.1}$$

The system is rearranged according to the appropriate boundary conditions:

$$A\tilde{x} = B\tilde{y} \tag{6.2}$$

where $\tilde{x}$ is the vector of the unknown boundary conditions and $\tilde{y}$ is the vector of the applied boundary conditions. The system is then solved as:

$$\tilde{x} = A^{-1}B\tilde{y} \tag{6.3}$$

resulting in wide solution due to the unconsidered dependency throughout the rows of $\tilde{x}$. To obtain sharp results, the two deterministic matrices are multiplied first and then post-multiplied by an interval vector to preserve interval dependency:

$$\tilde{x} = \left(A^{-1}B\right)\tilde{y} \tag{6.4}$$

In case H and G matrices cannot be computed exactly, numerical integration must be used resulting in an integration error. The error is considered in the latter chapter.

Chapter VII

Integration Error and Rounding Error

The following chapter describes the interval treatment of integration error. The integration scheme which is used to demonstrate the method is the polynomial expansion using Taylor series.

7.1 Taylor Series Expansion

In this work, Taylor series expansion (Taylor 1715) is considered as an example scheme for numerical integration. The integration error, which results from the approximation of the function by a finite series, is treated by an interval approach to ensure the guaranteed enclosure of the true error. Although a specific numerical integration scheme is considered as an example, the methodology can be extended to any numerical integration procedure. The following chapter develops the treatment of integration error in the boundary element method using interval concepts.

Any function can be expressed as a polynomial in terms of its derivatives at some point a using Taylor series expansion:

$$f(x) = \frac{f(a)}{0!} + \frac{f'(a)}{1!}(x-a) + \frac{f''(a)}{2!}(x-a)^2 + \ldots + \frac{f^m(a)}{m!}(x-a)^m \qquad (7.1)$$

where $m \to \infty$. If the function has a finite amount of nonzero derivatives, it can be integrated exactly:

$$\int_x f(x)dx = \int_x [\frac{f(a)}{0!} + \frac{f'(a)}{1!}(x-a) + \frac{f''(a)}{2!}(x-a)^2 + \ldots + \frac{f^n(a)}{n!}(x-a)^n]dx \qquad (7.2)$$

where n corresponds to the last nonzero derivative of the function. Since a function $f(x)$ is represented by a polynomial, its integration can be performed as:

$$\int_x f(x)dx = \left[f(a)x + \frac{f'(a)}{2}(x-a)^2 + \frac{f''(a)}{6}(x-a)^3 + ... + \frac{f^n(a)}{(n+1)!}(x-a)^{n+1} \right]_x \quad (7.3)$$

However, if the function has an infinite amount of nonzero derivatives, integration of the Taylor series introduces integration errors, since not all terms in the series can be accounted for.

7.2 Error Analysis on Taylor Series Expansion

Considering a function having an infinite number of nonzero derivatives, its expansion can still be expressed exactly by considering Taylor series expansion with remainder given as:

$$f(x) = \frac{f(a)}{0!} + \frac{f'(a)}{1!}(x-a) + \frac{f''(a)}{2!}(x-a)^2 + ... + \frac{f^{n-1}(a)}{(n-1)!}(x-a)^{n-1} + R_n \quad (7.4)$$

where n corresponds to the n^{th} derivative of the function and R_n is the series remainder:

$$R_n = \frac{f^n(\zeta)(x-a)^n}{n!} \qquad a < \zeta < x \quad (7.5)$$

Thus, any function can be integrated exactly as:

$$\int_x f(x)dx = \int_x [\frac{f(a)}{0!} + \frac{f'(a)}{1!}(x-a) + \frac{f''(a)}{2!}(x-a)^2 + ... + \frac{f^{n-1}(a)}{(n-1)!}(x-a)^{n-1} + R_n]dx$$

(7.6)

Hence, integration error $\int_x R_n dx$ can be defined:

$$\int_x R_n dx = \int_x f(x)dx - \int_x [\frac{f(a)}{0!} + \frac{f'(a)}{1!}(x-a) + \frac{f''(a)}{2!}(x-a)^2 + ... + \frac{f^{n-1}(a)}{(n-1)!}(x-a)^{n-1}]dx \tag{7.7}$$

Integrating Eq. (7.5) yields:

$$\int_x R_n dx = \frac{f^n(\zeta)(x-a)^{n+1}}{(n+1)!}\Bigg|_{x_1}^{x_2} \tag{7.8}$$

However, the closed form solution of $\int_x R_n dx$ cannot be obtained since ζ in general is unknown and therefore the minimum and the maximum values of the integration error are computed.

$$\min\left\{\int_x R_n dx\right\} = \min\left\{\frac{f^n(\zeta)(x-a)^{n+1}}{(n+1)!}\Bigg|_{x_1}^{x_2}\right\}, \quad a \le \zeta \le x \tag{7.9}$$

$$\max\left\{\int_x R_n dx\right\} = \max\left\{\frac{f^n(\zeta)(x-a)^{n+1}}{(n+1)!}\Bigg|_{x_1}^{x_2}\right\}, \quad a \le \zeta \le x \tag{7.10}$$

Having the extreme bounds on the integration error, the integration error can be expressed as an interval number:

$$\tilde{\tilde{E}} = \left[\min\left\{\int_x R_n dx\right\}, \max\left\{\int_x R_n dx\right\}\right] \tag{7.11}$$

However, for high precision numerical integration, the integration error will be small compared to the smallest machine number. In this case, the absolute value of the lower and upper bounds are numerically close to each other, and the true lower and upper error

bounds may be ambiguous. To ensure that the correct bounds are enclosed, the error is bounded using the maximum absolute value of the remainder as (Zalewski et al. 2006):

$$\tilde{\tilde{E}}_{Integration} = \max\left\{ abs\left[\frac{f^{n}(\zeta)(x-a)^{n+1}}{(n+1)!}\Bigg|_{x_1}^{x_2} \right] \right\}[-1,1] \;,\; a \le \zeta \le x \tag{7.12}$$

Also, using $\frac{m}{2}$ point integration based on the Taylor series expansion, where m is an even positive real number, results in the approximate terms of the H and G matrices computed as:

$$\int_x f(x)dx = \int_x \left[\sum_{n=1}^{m} \frac{f^{n-1}(a)}{(n-1)!}(x-a)^{n-1} \right] dx = \left[\sum_{n=1}^{m} \frac{f^{n-1}(a)}{(n)!}(x-a)^{n} \right]_{x_1}^{x_2} \tag{7.13}$$

7.3 Interval Boundary Element Method Formulation Considering Integration Error

Eq. (7.12) obtains the bounds on the integration error for Taylor series expansion. However, the equation becomes trivial if the absolute value of the minimum or maximum of the remainder approaches infinity. This is the case for the diagonal matrix coefficients of the G matrix and therefore they require a special treatment. Also the diagonal coefficients of the H matrix require special consideration since their integral is zero and therefore the integration error is zero for those terms.

In considering the integration error in IBEM, the approximate values of all matrix coefficients are first evaluated using Eq. (7.13). The integration error bounds of the non-diagonal coefficients of the H and G matrices are computed using Eq. (7.12). The integral and therefore the integration error of the diagonal terms of the H matrix are zero as described previously. The interval diagonal coefficients of the H matrix are computed

such that matrix H encloses a singular matrix and therefore it satisfies the boundary element formulation. This requires that at least one boundary value of the potential is known for the problem to have a unique solution.

The diagonal coefficients of the G matrix contain singular integrals, as the distance $r = |x - \xi|$ from Eq. (2.7) vanishes at the node. This is due to the choice of the weighting function to be the Green's function in the boundary element formulation. The approximate value of the diagonal coefficients is computed using Eq. (7.13). Since the function is singular at the node, $\max\left\{abs\left[f^{n}(\zeta)\right]\right\}$ becomes infinite and Eq. (7.12) cannot be used to meaningfully determine the error bounds. Therefore, the closed form solution of the improper integral of the diagonal coefficients of the G matrix is found, which is not necessarily in the domain of the actual integration over an element. The integration domain of the closed form improper integral is found from the explicit integration tables and is integral dependent. The integration domain of the element is determined from the coordinates of its endpoints. If the domain of the improper integral is equal to that of the element, the difference between the closed form solution and the numerical integration is considered as the integration error. Due to the same numerical considerations as in the previous section, symmetric interval bounds are then found as:

$$\tilde{\tilde{E}}_{Integration} = \left(\int_{x_1}^{x_2} f(x)dx - \left[\sum_{n=1}^{m} \frac{f^{n-1}(a)}{(n)!}(x-a)^{n} \right]_{x_1}^{x_2} \right)[-1,1] \tag{7.14}$$

If the domain of the improper integral is different than that of the element, the remaining domain is integrated numerically using Eq. (7.13) and the error found using Eq. (7.12).

The IBEM formulation results in interval non-diagonal matrix coefficients for H and G matrices computed as:

$$\left[\sum_{n=1}^{m}\frac{f^{n-1}(a)}{(n)!}(x-a)^n\right]\Bigg|_{x_1}^{x_2}+\max\left\{abs\left[\frac{f^n(\zeta)(x-a)^{n+1}}{(n+1)!}\Bigg|_{x_1}^{x_2}\right]\right\}[-1,1]\ ,\ a\le\zeta\le x \quad (7.15)$$

The diagonal coefficients of the G matrix are computed as following:

$$\left[\sum_{n=1}^{m}\frac{f^{n-1}(a)}{(n)!}(x-a)^n\right]\Bigg|_{x_1}^{x_2}+\left(\int_x f(x)dx-\left[\sum_{n=1}^{m}\frac{f^{n-1}(a)}{(n)!}(x-a)^n\right]\Bigg|_x\right)[-1,1]$$
$$\max\left\{abs\left[\frac{f^n(\zeta)(x-a)^{n+1}}{(n+1)!}\Bigg|_x^{x_2}\right]\right\}[-1,1]+\max\left\{abs\left[\frac{f^n(\zeta)(x-a)^{n+1}}{(n+1)!}\Bigg|_{x_1}^{x}\right]\right\}[-1,1]\ ,\ a\le\zeta\le x \quad (7.16)$$

Eq. (7.15) and Eq. (7.16) can be rewritten as:

$$\int_x \hat{f}(x)dx+\tilde{\tilde{E}}_{Integration} \quad (7.17)$$

Where $\int_x \hat{f}(x)dx$ is the numerical integration of $\int_x f(x)dx$. The diagonal coefficient of the H matrix, where $H\in\Re^{nxn}$, are computed from the boundary element formulation as:

$$H_{ii}=-\sum_{j=1,\,j\neq i}^{n}H_{ij} \quad (7.18)$$

Hence, interval boundary element analysis (IBEA), using the interval bounds on the integration error is performed resulting in:

$$\tilde{\tilde{H}}\tilde{\tilde{u}}=\tilde{\tilde{G}}\tilde{\tilde{q}} \quad (7.19)$$

Eq. (7.19) is rearranged according to the appropriate boundary conditions:

$$\tilde{\tilde{A}}\tilde{\tilde{x}}=\tilde{\tilde{b}} \quad (7.20)$$

The interval linear system of equation can be solved using the iterative methods described in the previous chapters. The rounding error (Alefeld 1983, Gay 1982, Hansen 1965, Jannson 1990, Neumaier 1987, Neumaier 1989, Neumaier 1990, Rump 1990, Rump 2001, Sunaga 1958) can be implemented into the interval solver.

Chapter VIII

Discretization Error

Chapter VIII develops the boundary element formulation to account for discretization error using interval concepts.

8.1 Interval Treatment of the Discretization Error

The discretization error in the solutions to integral equations results from considering a finite number of points for which the solutions are computed. In general, the true solutions to integral equations are functions, not discrete values, and therefore the space of the approximate solutions does not cover the space of the true solutions. The boundary integral equations can be obtained by the use of point collocation methods resulting in equation of the form of Eq. (2.14). The boundary integral equations are satisfied exactly only if all the locations of the source point ξ on the boundary are considered. However, to obtain a linear system of equations, a finite amount of source points is considered. Moreover, the location of the source points is unique and the solution is considered as a polynomial interpolation between the discrete values whose location corresponds to the location of the source point. This allows for the linear system of equations to be unique and thus the system can be solved for the unknown boundary values. It should be noted that if all source points are considered, the boundary values at all points can be computed, resulting in the true solution. The boundary integral equation can also be evaluated over n sub-domains as expressed by Eq. (2.17). The unique

location of the source point and its correspondence to the point at which the approximate solution is computed must be satisfied for all sub-domains. Eq. (2.17) is satisfied exactly only if all the locations of the source point are considered. Thus the discretization error is introduced in the same manner as in Eq. (2.14).

In the analysis of the discretization error, all the locations of the source point in the continuous boundary integral equation:

$$\frac{1}{2}u(\xi) + \int_{\Gamma} q^{*}(x,\xi)u(x)dx = \int_{\Gamma} u^{*}(x,\xi)q(x)dx, \quad \xi \in \Gamma \tag{8.1}$$

are treated via interval approach. The existence and uniqueness of the solution to the above problem for two dimensional Laplace equation when u or q, but not both, is given, is well studied (Friedman 1976). Considering interval bounds on all the possible locations of the source points allows obtaining interval solutions which enclose the true solution. From the interval bounds on the boundary values, the bounds on the true solution for any point in the domain can be computed. Eq. (8.1) is bounded by an interval boundary integral equation in which the terms $u^{*}(x,\xi)$ and $q^{*}(x,\xi)$ are enclosed by known interval-valued functions. The unknown functions $u(x)$ and $q(x)$ in Eq. (8.1) are then bounded by interval values enclosing the true solution.

The integral over the domain can be expressed as the sum of the integrals over the elements, Eq. (2.17), and thus the boundary integral equation must be bounded on each element for all the locations of the source points. Hence, for the boundary Γ is

subdivided into n boundary elements and for each element j the interval values $\tilde{u}$ and $\tilde{q}$ that bound the functions $u(x)$ and $q(x)$ are found (Figure 8.1).

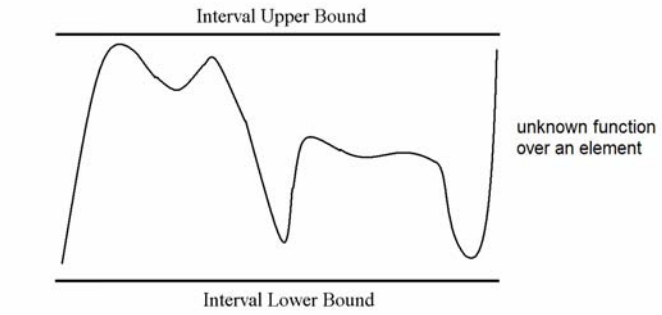

Figure 8.1. Interval bounds on a function.

It is assumed that on all other elements except for the element in consideration the bounds on all boundary values are known. Also either the Dirichlet or the Neumann boundary condition bounds are known for the element in consideration and the remaining boundary value for the single element in consideration is enclosed. The process is repeated for the second element with the assumed bounds for all the other elements, a computed bound for the previously considered element, and either the Dirichlet or the Neumann boundary condition bounds for the second element in consideration. This procedure known as the interval Gauss-Seidel iteration is performed for all elements until the true solution is enclosed. Mathematically the above statement can be expressed as:

$\forall j \in \{1,2,...,n\}$ *Assume* $\underline{u_i} \le u_i \le \overline{u_i}$, $\underline{q_i} \le q_i \le \overline{q_i}$ *is known* $\forall i \ne j$.

Also known $\underline{q_j} \le q_j \le \overline{q_j}$. *Find* $\underline{u_j} \le u_j \le \overline{u_j}$

$$\forall \xi_j \left| \begin{array}{l} \frac{1}{2}u(\xi_j) + \int_{\Gamma_j} q^*(x,\xi_j)u_j(x)d\Gamma_j = \\ \sum_{i=1,i\ne j}^{n} \int_{\Gamma_i} u^*(x,\xi_j)q_i(x)d\Gamma_i + \int_{\Gamma_j} u^*(x,\xi_j)q_j(x)d\Gamma_j - \sum_{i=1,i\ne j}^{n} \int_{\Gamma_i} q^*(x,\xi_j)u_i(x)d\Gamma_i \end{array} \right.$$

Or

$\forall j \in \{1,2,...,n\}$ *Assume* $\underline{u_i} \le u_i \le \overline{u_i}$, $\underline{q_i} \le q_i \le \overline{q_i}$ *is known* $\forall i \ne j$.

Also known $\underline{u_j} \le u_j \le \overline{u_j}$. *Find* $\underline{q_j} \le q_j \le \overline{q_j}$

$$\forall \xi_j \left| \begin{array}{l} \int_{\Gamma_j} u^*(x,\xi_j)q_j(x)d\Gamma_j = \frac{1}{2}u(\xi_j) + \int_{\Gamma_j} q^*(x,\xi_j)u_j(x)d\Gamma_j + \\ \sum_{i=1,i\ne j}^{n} \int_{\Gamma_i} q^*(x,\xi_j)u_i(x)d\Gamma_i - \sum_{i=1,i\ne j}^{n} \int_{\Gamma_i} u^*(x,\xi_j)q_i(x)d\Gamma_i \end{array} \right. \quad (8.2)$$

Each term of the summation in Eq. (8.2) is represented graphically (Figure 8.2).

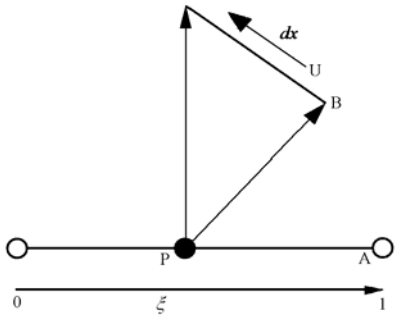

Figure 8.2. Integration from element B from point P on element A.

If u or q are specified boundary conditions, the interval integration can be performed explicitly as described in the previous section. In this work, for computational purposes, the system is solved using Krawczyk iteration rather than using the interval Gauss-Seidel iteration. This substitution of the method for bounding the unknown boundary values can be made since both of these methods are iterative methods for

solving interval linear systems of equations and both obtain guaranteed bounds for the solution. Hence, the formulation of the interval boundary integral equations for the IBEM is performed such that the resulting interval linear system of equations is of the form of Eq. (4.25).

Chapter IX

Kernel Splitting Technique

Chapter IX describes the development of the interval kernel splitting technique to enclose the interval Fredholm equation of the first kind. The enclosed interval equations are then solved using boundary element formulation. Since the resulting interval boundary integral equations enclose the continuous interval equations, their solutions enclose the solutions to the continuous problem.

9.1 Interval Kernel Splitting Technique

The analysis of the discretization error requires that the boundary integral equations for each element be enclosed for all the locations of the source point ξ. The integral equations in the boundary element formulation are of the form of the Fredholm equation of the first kind (Fredholm 1903). Kernel splitting techniques have been used to enclose the Fredholm equation of the first kind in which the right side is deterministic (Dobner 2002) as:

$$\int_{\Gamma} \tilde{a}(x,\xi)u(x)d\Gamma = b(\xi) \tag{9.1}$$

However, the interval boundary integral equations considered herein have an interval right side, due to the interval location of the source point $\tilde{\xi}$, and therefore a new interval kernel splitting technique (IKST) is developed (Zalewski and Mullen 2008).

Theorem 4.

Let $k \in \Re^{n\times n}$, $\xi \in \Re^n$, $x \in \Re^n$, *and* $b \in \Re^n$ *be given.*
If $\int_\Gamma k(x,\tilde{\xi})u(x)dx = b(\tilde{\xi}), \forall \xi \in \tilde{\xi} = \left[\underline{\xi}, \overline{\xi}\right]$

then $\left[\int_{\Gamma_1} k(x,\tilde{\xi})dx\tilde{u} + \int_{\Gamma_2} \tilde{k}dx\tilde{u}\right] \supseteq \left[\int_\Gamma k(x,\tilde{\xi})u(x)dx = b(\tilde{\xi})\right], \forall \xi \in \tilde{\xi} = \left[\underline{\xi}, \overline{\xi}\right]$

$$\left|\begin{array}{l} k(x,\tilde{\xi})\big|_{\Gamma_1} > 0 \text{ or } k(x,\tilde{\xi})\big|_{\Gamma_1} < 0,\ k(x,\tilde{\xi})\big|_{\Gamma_2} \in 0,\ \bigcup_{i=1}^{2}\Gamma_i = \Gamma,\ \bigcap_{i=1}^{2}\Gamma_i = 0 \text{ and} \\ \tilde{k} = [\min\{k(x+\tilde{\varepsilon},\tilde{\xi})\}, \max\{k(x+\tilde{\varepsilon},\tilde{\xi})\}], \forall \varepsilon \in \tilde{\varepsilon} = [-\varepsilon, \varepsilon] \end{array}\right.$$

Proof: The integral of the product of two functions is enclosed considering interval bounds on the unknown value as:

$$\int_\Gamma a(x,\tilde{\xi})\tilde{u}dx \supseteq \int_\Gamma a(x,\tilde{\xi})u(x)dx = b(\tilde{\xi}) \tag{9.2}$$

To separate the kernels such that the unknown $\tilde{u}$ can be taken out of the integral on Γ, the left side integral from Eq. (9.2) is expressed as a sum of the integrals:

$$\int_\Gamma a(x,\tilde{\xi})\tilde{u}d\Gamma = \int_{\Gamma_1} a(x,\tilde{\xi})\tilde{u}dx + \int_{\Gamma_2} a(x,\tilde{\xi})\tilde{u}dx \tag{9.3}$$

where: $\bigcup_{i=1}^{n}\Gamma_i = \Gamma$ and $\bigcap_{i=1}^{n}\Gamma_i = 0$ and:

$$a(x,\tilde{\xi}) > 0 \quad \text{or} \quad a(x,\tilde{\xi}) < 0 \quad on\ \Gamma_1 \tag{9.4}$$

$$a(x,\tilde{\xi}) \in 0 \qquad on\ \Gamma_2 \tag{9.5}$$

The interval kernel is of the same sign on Γ_1, thus $\tilde{u}$ can be taken out of the integral on Γ_1:

$$\int_{\Gamma_1} a(x,\tilde{\xi})\tilde{u}dx = \int_{\Gamma_1} a(x,\tilde{\xi})dx\tilde{u} \tag{9.6}$$

Due to the subdistributive property of interval numbers, $\tilde{u}$ cannot be taken out of the integral on Γ_2. The direct application of the subdistributive property may result in inner bounds on the interval integral as:

$$\int_{\Gamma_2} a(x,\tilde{\xi})dx\tilde{u} \subseteq \int_{\Gamma_2} a(x,\tilde{\xi})\tilde{u}dx \tag{9.7}$$

Hence the interval kernel is bounded by its limits on Γ_2:

$$\int_{\Gamma_2} \tilde{a}\tilde{u}dx \supseteq \int_{\Gamma_2} a(x,\tilde{\xi})\tilde{u}dx \tag{9.8}$$

where $\tilde{a}$ is defined as:

$$\tilde{a} = [\min\{a(x+\tilde{\varepsilon},\tilde{\xi})\}, \max\{a(x+\tilde{\varepsilon},\tilde{\xi})\}] \tag{9.9}$$

$$\tilde{\varepsilon} = [-\varepsilon, \varepsilon] \tag{9.10}$$

ε is the tolerance level of the nonlinear solver used to find the zero location of $a(x,\tilde{\xi})$. In order to show that enclosing the kernel function by $\tilde{a}$ on Γ_2 allows $\tilde{u}$ to be taken out from the integral on Γ_2, the integral on Γ_2 is expressed as an infinite sum:

$$\int_{\Gamma_2} \tilde{a}\tilde{u}dx = \lim_{\Delta x\to 0}\sum_{i=1}^{n}(\Delta x\tilde{a}\tilde{u})\Big|_{\Gamma_2} = \lim_{\Delta x\to 0}(n\Delta x\tilde{a}\tilde{u})\big|_{\Gamma_2} = \lim_{\Delta x\to 0}(n\Delta x\tilde{a})\tilde{u}\big|_{\Gamma_2} = \lim_{\Delta x\to 0}\sum_{i=1}^{n}(\Delta x\tilde{a})\Big|_{\Gamma_2}\tilde{u} = \int_{\Gamma_2}\tilde{a}dx\tilde{u} \tag{9.11}$$

where Δx is a small part of Γ_2. Thus $\tilde{u}$ can be taken out of both integrals on Γ_1 and on Γ_2 and the split interval boundary integral equation becomes:

$$\int_{\Gamma_1} a(x,\tilde{\xi})dx\tilde{u} + \int_{\Gamma_2} \tilde{a}dx\tilde{u} \supseteq \int_{\Gamma} a(x,\tilde{\xi})\tilde{u}dx \supseteq \int_{\Gamma} a(x,\tilde{\xi})u(x)dx = b(\tilde{\xi}) \tag{9.12}$$

The kernels are bounded for all the elements resulting in interval linear system of equations:

$$\tilde{A}_1\tilde{u} + \tilde{A}_2\tilde{u} \supseteq \tilde{b} \tag{9.13}$$

Therefore, the IKST bounds the continuous boundary integral equation for all the locations of the source point ξ and Eq. (8.1) is guaranteed to be satisfied for all the weighted residual functions.

Chapter X

Interval Boundary Element Method Formulation Considering Discretization Error

Chapter X describes the interval boundary element formulation to account for the discretization error using the concepts described and developed in the previous chapters. A correct system parameterization is considered to obtain a unique solution and realistic interval enclosure.

10.1 Interval Treatment of Discretization Error in Boundary Element Analysis

The previous sections described the treatment of the discretization error via interval methods. This section provides the IBEM formulation considering the discretization error (Zalewski and Mullen 2008). In order to obtain a true solution to the boundary integral equation, the integral equation must be satisfied for all weighted residual functions in the point collocation method, i.e. the integral equation must be satisfied for all locations of the source points ξ. Each source point must have a unique location on an individual element to obtain a unique linear system of equations. Furthermore, the source point must have the same location on any particular element throughout the rows of the H and G matrices, which are in $\Re^{nxn}$. Direct interval approach considers the location of the source point on the entire element and thus allows two source points to share the same location on two adjacent elements. Naive interval analysis does not consider a unique location of the source point on an individual element, resulting in the reduction of the rank of the system of equations. Also, since the kernel

functions are nonlinear functions of ξ, the location of the source point cannot be directly taken out of the integral. Thus, the interval bounds on the location of the source point $\tilde{\xi}$ are subdivided to increase the dependency of their location on an individual element and to satisfy the uniqueness of the location of each source point to obtain n independent equations. For convenience, the system is parameterized such that $\tilde{\xi} = [0,1]$ is the location of the source point that is scaled according to the length of each element. In performing interval matrix products, the value of $\tilde{\xi}$ is decomposed into subintervals such that:

$$\bigcup_{i=1}^{n} \tilde{\xi}_i = \tilde{\xi}, \ \ and \ \bigcap_{i=1}^{n} \tilde{\xi}_i = 0 \tag{10.1}$$

The parameterized boundary integral equation is enclosed using IKST for each subinterval $\tilde{\xi}_i$, resulting in the linear system of equations:

$$H_1(\tilde{\xi}_i)\tilde{u} + H_2(\tilde{\xi}_i)\tilde{u} = G_1(\tilde{\xi}_i)\tilde{q} + G_2(\tilde{\xi}_i)\tilde{q} \tag{10.2}$$

where the kernel is either positive or negative for $H_1(\tilde{\xi}_i)$ and $G_1(\tilde{\xi}_i)$ and contains zero for $H_2(\tilde{\xi}_i)$ and $G_2(\tilde{\xi}_i)$. The system of equations is rearranged according to the boundary conditions yielding:

$$A_1(\tilde{\xi}_i)\tilde{x} + A_2(\tilde{\xi}_i)\tilde{x} = b_1(\tilde{\xi}_i) \tag{10.3}$$

The resulting Eq. (10.3) is solved using a parametric interval equation solver described in Chapter V with a preconditioning matrix being an identity matrix I which numerically gave the sharpest results.

Chapter XI: Discretization Error for Domains with Flux Singularities

The following chapter develops the treatment of flux singularities in interval boundary element formulation for the analysis of the discretization error. Interval enclosure of the true solution is considered on all the boundaries except for the portion at which a flux singularity occurs for which the strength of the singularity is bounded.

11.1 Interval Boundary Element Formulation for Systems with Flux Singularities

Enclosing the exact solution using the methods described in the previous chapters leads to infinite bounds for systems whose true solution is singular at some point. The algorithms to solve the interval linear system of equations, chapter V, consider bounds on all unknown variables and therefore if one of them is infinite, the resulting bounds will be infinite for all the unknown variables. This section describes the interval treatment of geometrically induced flux singularities such that meaningful discretization error bounds can be obtained for all the unknown variables except for the one at which the singularity occurs.

In engineering problems, singular flux solutions are generated by the geometry of the system such as a reentrant corner or a slit such as crack in engineering mechanics. Despite the presence of the singularity, the continuous boundary integral equation is still satisfied. For simplicity the boundary is taken to be along the x direction resulting in a boundary integral equation of the following form:

$$\frac{1}{2}u(\xi)+\int_{\Gamma_x} q^*(x,\xi)u(x)dx=\int_{\Gamma_x} u^*(x,\xi)q(x)dx \tag{11.1}$$

Let us assume that the true solution to a flux on part of boundary Γ_1 is singular. Thus, treating Eq. (11.1), with an interval approach described in previous chapters, results in infinite bounds as described above. The integral on the right side of Eq. (11.1) is separated to isolate the singular terms.

$$\frac{1}{2}u(\xi)+\int_{\Gamma_x} q^*(x,\xi)u(x)dx=\int_{\Gamma_x-\Gamma_1} u^*(x,\xi)q(x)dx+\int_{\Gamma_1} u^*(x,\xi)q(x_{singular})dx \tag{11.2}$$

Eq. (11.2) can be discretized following the boundary element formulation as:

$$\begin{aligned}\frac{1}{2}u_i+\sum_{Elements}\int_{\Gamma_x} q^*(x,\xi)\Phi(x)dxu_i=&\sum_{Elements}\int_{\Gamma_x-\Gamma_1} u^*(x,\xi)\Phi(x)dxq_i\\&+\sum_{Elements}\int_{\Gamma_1} u^*(x,\xi)\Phi(x)dxq_{i\,singular}\end{aligned} \tag{11.3}$$

To eliminate the effect of the singular flux solution on boundary Γ_1, such that meaningful interval bounds can be computed, the original shape function for the singular flux element is replaced by a new shape function consisting of the original shape function multiplied by the strength of the singularity. The strength of the singularity can be found by satisfying zero Dirichlet boundary conditions, for a solution which is singular at a point, for a correct geometry which induces the same singularity as encountered in the problem. To obtain the strength of the singularity for the Laplace problem, one needs to solve:

$$u=r^m\sin(m\theta) \tag{11.4}$$

where r is the distance from the singularity, θ is the angle from the horizontal, and m is the strength of the singularity which is obtained from satisfying the boundary conditions

for an appropriate geometry. Multiplying the original shape function $\Phi(x)$ by the singularity strength found from Eq. (11.4) results in the singular flux $q_{singular}$ to be replaced by a finite flux intensity factor $\hat{q}$. Thus Eq. (11.3) can be rewritten as (Mikhlin 1965, Samko 2002, Zalewski and Mullen 2008):

$$\frac{1}{2}u_i + \sum_{Elements}\int_{\Gamma_x} q^*(x,\xi)\Phi(x)dx u_i = \sum_{Elements}\int_{\Gamma_x-\Gamma_1} u^*(x,\xi)\Phi(x)dx q_i + \sum_{Elements}\int_{\Gamma_1} u^*(x,\xi)\frac{\Phi(x)}{r(x)^m}dx\hat{q}_i \tag{11.5}$$

where $r(x)$ is the distance from singularity to any field point x and m is the strength of the singularity which depends on the geometry of the system and is known prior to the analysis by solving Eq. (11.4). It is important to note that $\hat{q}$ is not a value of the flux on boundary Γ_1 but rather it is the flux intensity factor, which is analogous to the stress intensity factor used in fracture mechanics. Eq. (11.5) is enclosed using parametric IKST resulting in the system of equations:

$$H_1(\tilde{\xi}_i)\tilde{u} + H_2(\tilde{\xi}_i)\tilde{u} = G_1(\tilde{\xi}_i)\tilde{\tilde{q}} + G_2(\tilde{\xi}_i)\tilde{\tilde{q}} \tag{11.6}$$

where the kernel is either positive or negative for $H_1(\tilde{\xi}_i)$ and $G_1(\tilde{\xi}_i)$ and contains zero for $H_2(\tilde{\xi}_i)$ and $G_2(\tilde{\xi}_i)$. Vector $\tilde{\tilde{q}}$ consists of the bounds on the nonsingular flux values as well as the bounds on flux intensity factors for the elements with singular flux value:

$$\tilde{\tilde{q}}_i = \tilde{q}_i \; on \; \Gamma_{x-1} \tag{11.7}$$

$$\tilde{\tilde{q}}_i = \tilde{\hat{q}}_i \; on \; \Gamma_1 \tag{11.8}$$

The system of equations is rearranged according to the boundary conditions yielding:

$$A_1(\tilde{\xi}_i)\tilde{\tilde{x}} + A_2(\tilde{\xi}_i)\tilde{\tilde{x}} = b_1(\tilde{\xi}_i) \tag{11.9}$$

Vector $\tilde{\tilde{x}}$ consists of the bounds on the nonsingular boundary values as well as the bounds on flux intensity factors for the elements with singular flux value. Eq. (11.9) is then solved using the interval equation solver described in Chapter V.

Chapter XII: Interval Bounds on the Solutions in the Domain of the System

Chapter XII describes the enclosures of the true solution in the domain of the system provided that the enclosure of the boundary values is guaranteed.

12.1 Enclosure of the Internal Potential Variable

The methods described in chapters VIII through XI obtain guaranteed enclosure of the solution on the boundary of the domain. The obtained boundary values, and possibly the applied boundary conditions, are interval numbers and therefore a special consideration needs to be given when computing internal variables. This chapter describes the treatment of the discretization error for the internal variables. It is assumed that the interval bounds for the boundary variables are computed using the methods presented in the previous chapters and therefore they guarantee the enclosure of the true solution on the boundary of the system. If the bounds on the boundary values are not guaranteed the enclosure of the true solution in the interior of the domain is not guaranteed either. In conventional boundary element analysis the internal potential is computed as:

$$u(\xi) = \int_{\Gamma} u^*(x,\xi) q(x) dx - \int_{\Gamma} q^*(x,\xi) u(x) dx, \quad \xi \in \Omega \tag{12.1}$$

where the location of the source point corresponds to the point at which the potential is to be calculated. If IBEM is used to compute interval bounds on all boundary values Eq. (12.1) is modified as:

$$\tilde{u}(\xi) = \int_{\Gamma} u^*(x,\xi)\tilde{q}dx - \int_{\Gamma} q^*(x,\xi)\tilde{u}dx, \quad \xi \in \Omega \tag{12.2}$$

where $\tilde{u}$ are the bounds on the boundary potentials, $\tilde{q}$ are the bounds on the boundary fluxes, and $\tilde{u}(\xi)$ is the bound on the internal potential. Direct integration of Eq. (12.2) may result in inner bounds on the true solution if the kernel functions change signs. This is a direct result of the subdistributive property of interval numbers, Eq. (4.12), and is analogous to the consideration given in developing IKST. Therefore, the domain of the integrals in Eq. (12.2) is separated such that the kernel functions, which are deterministic since the source point now has a prescribed location, are either positive or negative.

$$\tilde{u}(\xi) = \int_{\Gamma_1} u^*(x,\xi)\tilde{q}dx + \int_{\Gamma_2} u^*(x,\xi)\tilde{q}dx - \int_{\Gamma_1} q^*(x,\xi)\tilde{u}dx - \int_{\Gamma_2} q^*(x,\xi)\tilde{u}dx \tag{12.3}$$

where

$$u^*(x,\xi) \geq 0 \ \textit{and} \ q^*(x,\xi) \geq 0 \ \forall x \ \textit{on} \ \Gamma_1 \tag{12.4}$$

$$u^*(x,\xi) \leq 0 \ \textit{and} \ q^*(x,\xi) \leq 0 \ \forall x \ \textit{on} \ \Gamma_2 \tag{12.5}$$

Separating the integrals in such form also allows taking out the interval bounds out of the integrals without violating the subdistributive property as in IKST:

$$\tilde{u}(\xi) = \int_{\Gamma_1} u^*(x,\xi)dx\tilde{q} + \int_{\Gamma_2} u^*(x,\xi)dx\tilde{q} - \int_{\Gamma_1} q^*(x,\xi)dx\tilde{u} - \int_{\Gamma_2} q^*(x,\xi)dx\tilde{u} \tag{12.6}$$

Eq. (12.6) can be written in matrix form as:

$$\tilde{u}(\xi) = G_1\tilde{q} + G_2\tilde{q} - H_1\tilde{u} - H_2\tilde{u} \tag{12.7}$$

It should be noted that Eq. (12.7) does not introduce any new overestimation since the interval integration is performed exactly in the form of matrix multiplication. The only overestimation occurs due to the computed boundary values.

12.2 Enclosure of the Internal Flux Variable

The following section describes the computation of the flux variables for a two dimensional Laplace equation. There is no loss of generality in the formulation and the Laplace equation is strictly used for illustrative purposes. The procedure can be readily extended to other linear elliptic problems. The conventional computation of the internal flux variables is performed as:

$$q_x(\xi) = \frac{1}{2\pi}\frac{\partial H}{\partial \zeta}u - \frac{1}{2\pi}\frac{\partial G}{\partial \zeta}q \tag{12.8}$$

$$q_y(\xi) = \frac{1}{2\pi}\frac{\partial H}{\partial \eta}u - \frac{1}{2\pi}\frac{\partial G}{\partial \eta}q \tag{12.9}$$

where ζ and η are variables in the x and y directions, respectively. The partial derivative terms for the Laplace problem are given as:

$$\frac{\partial H}{\partial \zeta} = \int_{\Gamma} \frac{(x-\zeta)^2 n_x + 2(x-\zeta)(y-\eta)n_y - (y-\eta)^2 n_x}{|x-\zeta|^4}\,dx \tag{12.10}$$

$$\frac{\partial H}{\partial \eta} = \int_{\Gamma} \frac{(y-\eta)^2 n_y + 2(x-\zeta)(y-\eta)n_x - (x-\zeta)^2 n_y}{|x-\zeta|^4}\,dx \tag{12.11}$$

$$\frac{\partial G}{\partial \zeta} = -\int_{\Gamma} \frac{(x-\zeta)}{|x-\zeta|^2}\,dx \tag{12.12}$$

$$\frac{\partial G}{\partial \eta} = -\int_{\Gamma} \frac{(y-\eta)}{|x-\zeta|^2}\,dx \tag{12.13}$$

where ζ and η are components of the ξ vector determining the location of the source point such that $\xi = \langle \zeta, \eta \rangle$, x and y are components of the position vector to the boundary of the system describing the location of the filed point for each element and are variables, and n_x and n_y are components of the outward normal vector to the boundary of the system. The boundary values computed using IBEM are interval numbers and therefore Eq. (12.8) and Eq. (12.9) cannot be used to directly calculate the internal flux values due to the subdistributive property. Thus, the domain of the integrals of the kernel functions is separated such that the kernel functions, Eq. (12.10) – Eq. (12.13), which are deterministic, are either positive or negative. This leads to the bounds on the internal fluxes to be expressed as:

$$\tilde{q}_x(\xi) = \frac{1}{2\pi}\left(\left.\frac{\partial H}{\partial \zeta}\right|_{\Gamma_1} \tilde{u} + \left.\frac{\partial H}{\partial \zeta}\right|_{\Gamma_2} \tilde{u} \right) - \frac{1}{2\pi}\left(\left.\frac{\partial G}{\partial \zeta}\right|_{\Gamma_1} \tilde{q} + \left.\frac{\partial G}{\partial \zeta}\right|_{\Gamma_2} \tilde{q} \right) \tag{12.14}$$

$$\tilde{q}_y(\xi) = \frac{1}{2\pi}\left(\left.\frac{\partial H}{\partial \eta}\right|_{\Gamma_1} \tilde{u} + \left.\frac{\partial H}{\partial \eta}\right|_{\Gamma_2} \tilde{u} \right) - \frac{1}{2\pi}\left(\left.\frac{\partial G}{\partial \eta}\right|_{\Gamma_1} \tilde{q} + \left.\frac{\partial G}{\partial \eta}\right|_{\Gamma_2} \tilde{q} \right) \tag{12.15}$$

where the integrated kernel functions are positive on Γ_1 and negative on Γ_2. Eq. (12.14) and Eq. (12.15) can be written in matrix form as:

$$\tilde{q}_x(\xi) = H'_{1x}\,\tilde{u} + H'_{2x}\,\tilde{u} - G'_{1x}\,\tilde{q} - G'_{2x}\,\tilde{q} \tag{12.16}$$

$$\tilde{q}_y(\xi) = H'_{1y}\,\tilde{u} + H'_{2y}\,\tilde{u} - G'_{1y}\,\tilde{q} - G'_{2y}\,\tilde{q} \tag{12.17}$$

The computation of the internal variables does not require an interval equation solver but is performed by direct interval multiplication. The only overestimation of the internal solutions is due to the overestimation in the boundary values since the interval integration is performed exactly.

Chapter XIII: Example Problems

Chapter XIII presents numerical examples demonstrating the behavior of the interval bounds obtained using IBEM. All computations were performed using Matlab 6.5.1 code on a DELL LATITUDE D800 1.69 GHz Intel Pentium M processor having 512 MB of RAM and 74.4 GB of hard disk memory.

13.1 Interval Boundary Element Method Considering Uncertainty in the Boundary Conditions

The first example is a demonstration of the interval treatment of uncertain boundary conditions for the heat conduction problem expressed as a Laplace equation. The unit square domain of the problem as well as the boundary element mesh is shown (Figure 13.1). Nodes are located at the midpoint of each element. The left and right sides have a zero heat flux boundary condition while at the bottom the temperature is $[0,1]$ and at the top the temperature is $[1,2]$.

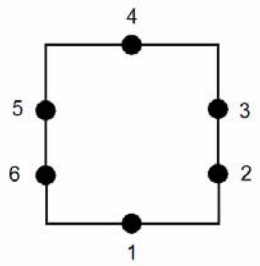

Figure 13.1. Boundary discretization of a unit square using six constant boundary elements.

The interval bounds are shown and compared with the combinatorial solution (Table 1) for the unknown boundary values. It should be noted that the interval solution is exact, which is attributed to the order of operation and the consideration of interval dependency. The two deterministic matrices are multiplied first and then post-multiplied by the interval vector as described in chapter VI.

Node Value	Lower Bound	Lower Bound with Parame-terization	Combina-torial Lower Bound	Combina-torial Upper Bound	Upper Bound with Parame-terization	Upper Bound
q1	-2.5770	-2.0763	-2.0763	0.0000	0.0000	0.5007
u2	0.0922	0.2451	0.2451	1.2451	1.2451	1.3981
u3	0.6019	0.7549	0.7549	1.7549	1.7549	1.9078
q4	-0.5007	0.0000	0.0000	2.0763	2.0763	2.5770
u5	0.6019	0.7549	0.7549	1.7549	1.7549	1.9078
u6	0.0922	0.2451	0.2451	1.2451	1.2451	1.3981

Table 1. Solutions to Laplace equation with uncertain boundary conditions for a six node mesh.

13.2 Interval Boundary Element Method Considering Integration Error

The second example considers integration error in IBEM to solve the heat transfer problem expressed in terms of Laplace equation of a 1:2 rectangular domain using six constant boundary elements with a node located at the mid-point (Figure 13.2). The sides of the domain have zero heat flux while the bottom is at zero temperature and a temperature of 50 is applied at the top. In this example, four point integration method

based on a Taylor series is used to develop interval terms in the H and G matrices. The interval system of equations is then solved using the developed solver from chapter V.

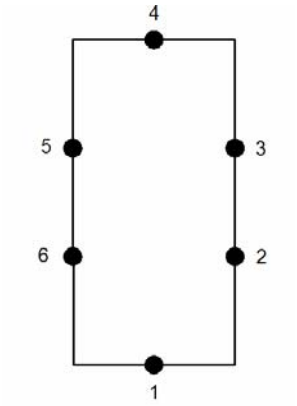

Figure 13.2. Boundary discretization of a rectangular domain using six constant boundary elements.

The solution obtained by exact integration is shown and compared to the bounds of the solution using the proposed method (Table 2).

Node Value	Lower Bound	Solution with exact integration	Upper Bound
q1	-33.6109	-28.1967	-24.0111
u2	11.1738	11.9357	12.4237
u3	37.5237	38.0643	38.8788
q4	23.5010	28.1967	34.1209
u5	37.5237	38.0643	38.8788
u6	11. 1738	11.9357	12.4237

Table 2. Solutions to Laplace in presence of integration error for a six node mesh.

13.3 Interval Boundary Element Method Considering Discretization Error

The third example obtains the bounds on the discretization error for the IBEA of the Laplace equation for the heat transfer within a unit square. The domain with zero heat flux on each side is considered as well as a zero temperature on the bottom and a unit temperature on the top. Five different meshes (Figure 13.3) are considered and the solutions in presence of the discretization error are compared. Ten subintervals are used in the computation since higher subdivision did not yield much improvement in the interval bounds.

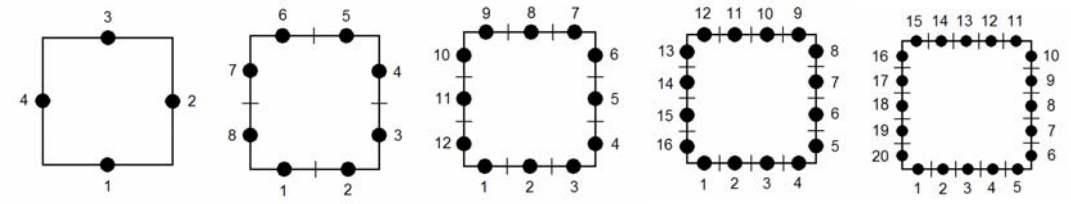

Figure 13.3. Constant boundary element discretization of a unit cube.

The bounds of the IBEA solution are shown and compared with an exact solution in the right lower corner for nodes 2, 3, 4, 5, 6 for the five respective meshes (Table 3) and the behavior of the effectivity index is shown for these nodes (Figure 13.4). Behavior of the interval bounds of the internal temperature for the middle segment of the cube located at $x = 0.5$ and stretching from $y = 0$ until $y = 1$ is shown, solid line, and compared with the true solution, dashed line, (Figure 13.5) for the 4, 8, and 12 element meshes as well as the behavior of the solution width of the internal temperature for these meshes (Figure 13.6). The behavior of the bounds on the internal heat flux in the x and y directions is shown for the same segment, solid line, and compared with the true solution, dashed line, (Figure 13.7, Figure 13.8).

Node Value	Lower Bound	Exact Lower Bound	Exact Upper Bound	Upper Bound	Middle Value	Width	Effective Width	Mid-point Node Solution
u2	-0.0221	0	1	1.0515	0.5147	1.0736	1.0736	0.5000
u3	-0.0244	0	0.5	0.5140	0.2448	0.5384	1.0769	0.2414
u4	-0.0213	0	1/3	0.3351	0.1569	0.3564	1.0693	0.1591
u5	-0.0232	0	0.25	0.2571	0.1170	0.2803	1.1210	0.1188
u6	-0.0233	0	0.2	0.2076	0.0921	0.2310	1.1548	0.0948

Table 3. Solutions to the Laplace equation in presence of dicretization error for a unit cube.

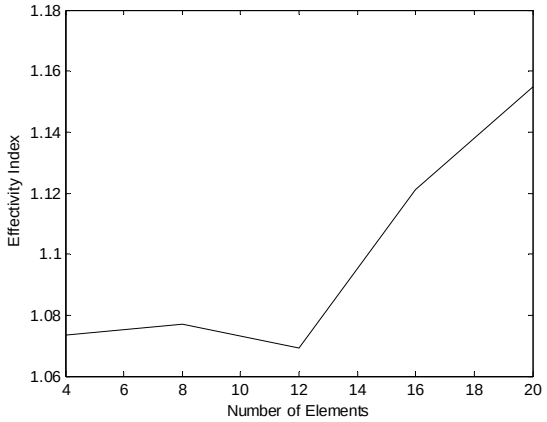

Figure 13.4. Behavior of the effectivity index with problem size.

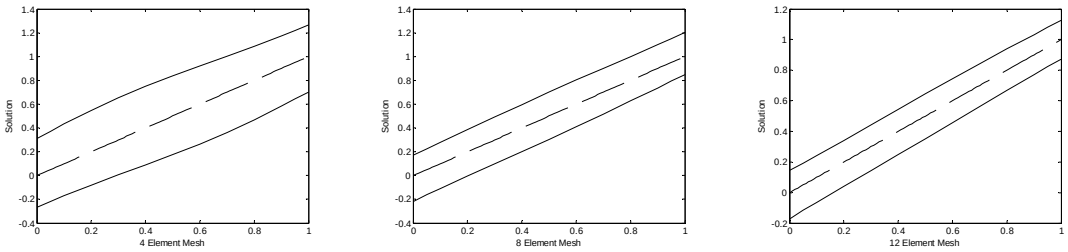

Figure 13.5. Behavior of the interval bounds for the interior temperature with mesh refinement.

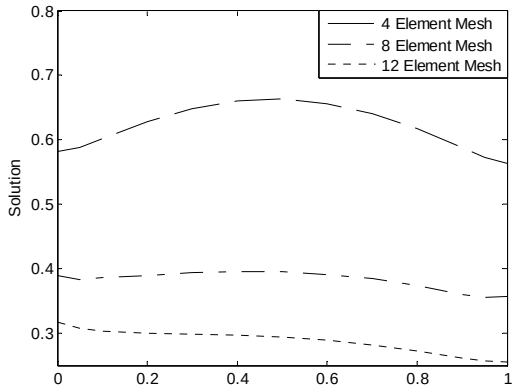

Figure 13.6. Behavior of the solution width for the interior temperature with problem size.

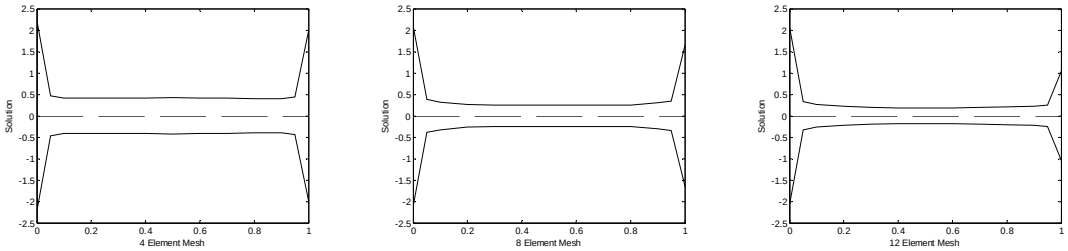

Figure 13.7. Behavior of the interval bounds for the interior x-direction heat flux with mesh refinement.

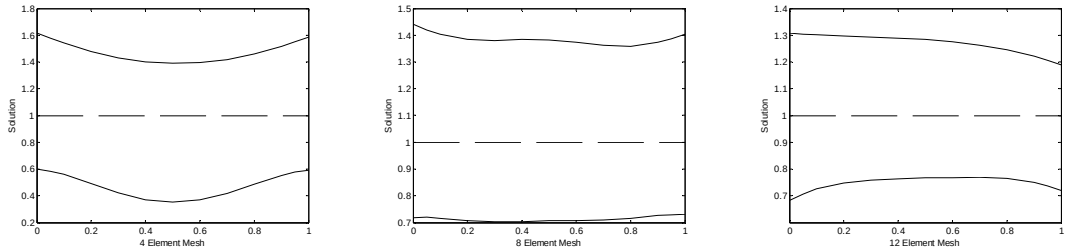

Figure 13.8. Behavior of the interval bounds for the interior y-direction heat flux with mesh refinement.

The fourth example demonstrates the convergence of the method with problem size by obtaining the bounds on the discretization error for the IBEA of the Laplace equation. A 1:2 ratio rectangular domain with zero heat flux on each side is considered as well as a zero temperature on the bottom and a unit temperature on the top. Five different meshes are considered (Figure 13.9) and the solutions in presence of the discretization error are compared. Ten subintervals were considered since further subdivision did not produce a significant improvement in the results.

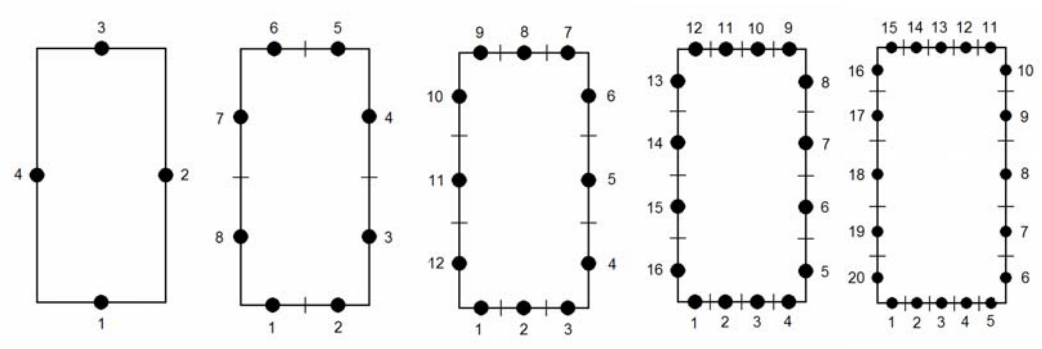

Figure 13.9. Boundary discretization using constant boundary elements for a rectangular domain.

The bounds of the IBEA solution are shown and compared with an exact solution in the right lower corner for nodes 2, 3, 4, 5, 6 for the five respective meshes (Table 4) and the behavior of the effectivity index is shown for these nodes (Figure 13.10).

Node Value	Lower Bound	Exact Lower Bound	Exact Upper Bound	Upper Bound	Middle Value	Width	Effective Width	Mid-point Node Solution
u2	-1.3943	0	1	2.7286	0.6671	4.1229	4.1229	0.5000
u3	-0.4278	0	0.5	0.8254	0.1988	1.2532	2.5064	0.2337
u4	-0.2561	0	1/3	0.5130	0.1285	0.7691	2.3073	0.1538
u5	-0.1849	0	0.25	0.3815	0.0983	0.5664	2.2655	0.1148
u6	-0.1433	0	0.2	0.3011	0.0789	0.4444	2.2222	0.0916

Table 4. Solutions to the Laplace equation in presence of dicretization error for a rectangular domain.

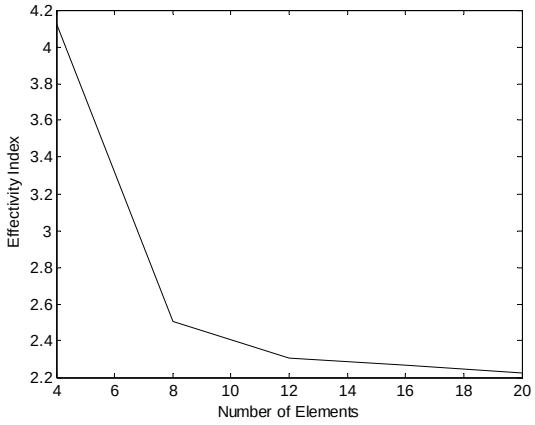

Figure 13.10. Convergence of the effectivity index with problem size for a rectangular domain.

13.4 Discretization Error Analysis Using Interval Boundary Element Method for a Torsion Problem

The fifth example illustrates the treatment of the discretization error for a torsion problem expressed in terms of the Laplace equation. A unit square domain with

appropriate Neumann boundary conditions, see Chapter III, applied on all boundaries is considered (Figure 13.11). The appropriate boundary conditions for the warping function, see Chapter III, are applied on the bottom boundary middle element: elements 2, 4, 6, 8 for the five respective meshes (Figure 13.11). Ten subintervals are considered in the simulations unless stated otherwise.

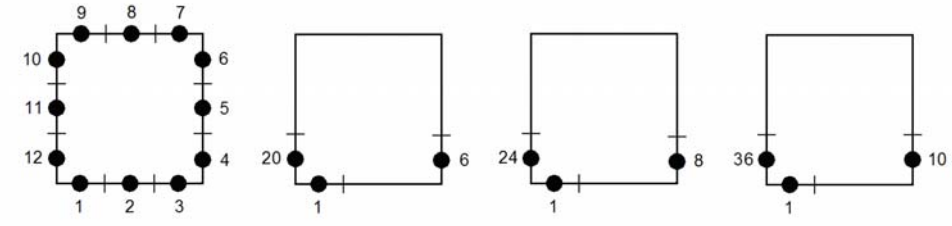

Figure 13.11. Boundary discretization using constant boundary elements for a torsion problem of a beam with a unit square cross section.

The widths of the solution (Figure 13.12), effectivity indices (Figure 13.13), and solution bounds, solid line, compared with the true solution, dashed line, (Figure 13.14) are compared for the right side bottom corner elements 4, 6, 8, and 10 (Figure 13.11) for the different meshes. Figure 13.15 shows the solution bounds of the right edge, solid line, compared with the true solution, dashed line. Figure 13.16 illustrates the convergence of the interval solution solid line, compared with the true solution, dashed line, with increased number of subintervals for node 4 in the 12 element mesh. Figure 13.17 shows the computational expense with increasing number of subintervals for the 36 element mesh. The computational cost of IBEM is depicted with increasing number of elements (Figure 13.18) and compared with the cubic regression (Figure 13.19). The ratio of the computational time necessary to perform IBEM versus the conventional BEM is compared with mesh size (Figure 13.20).

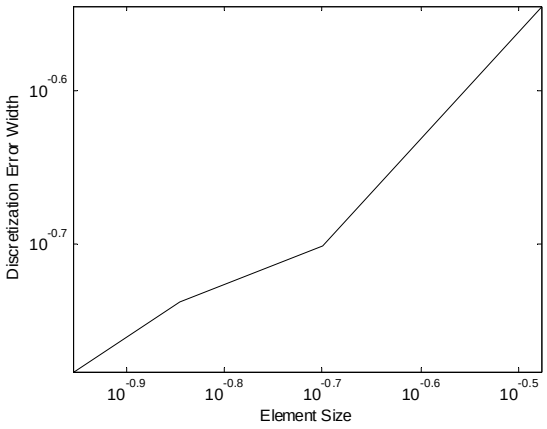

Figure 13.12. Behavior of the solution width with problem size.

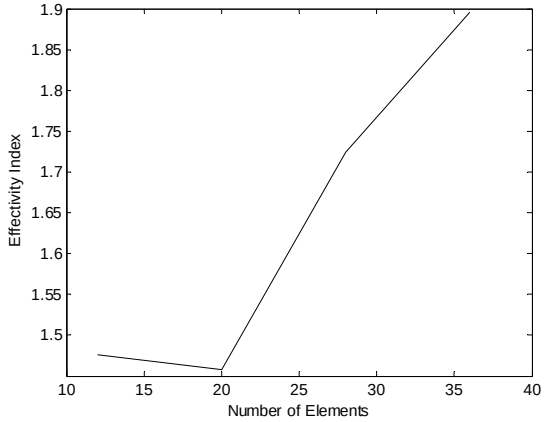

Figure 13.13. Behavior of the effectivity index with problem size.

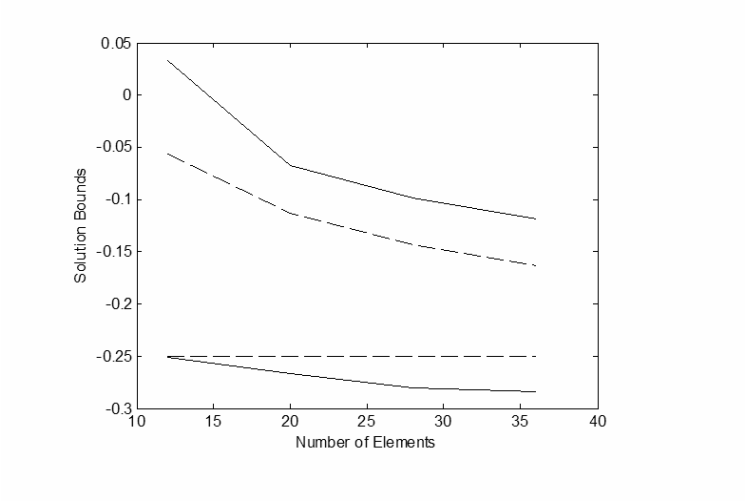

Figure 13.14. Behavior of the solution bounds with problem size.

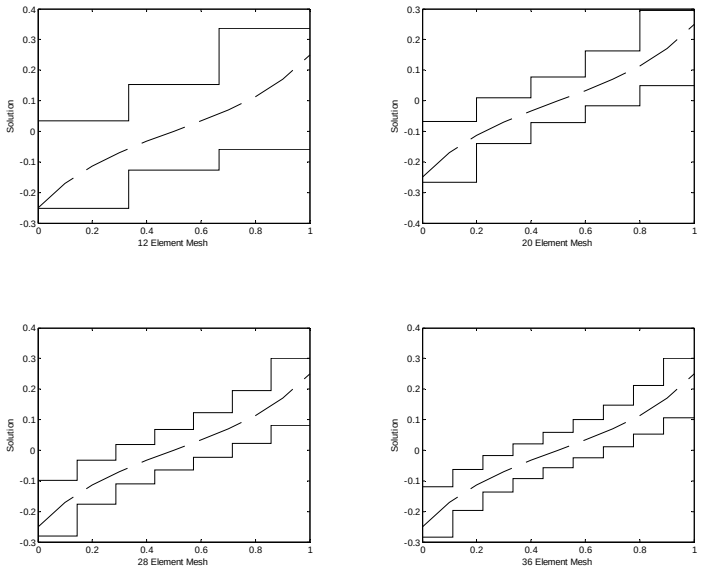

Figure 13.15. Behavior of the interval bounds for the different meshes on the right edge.

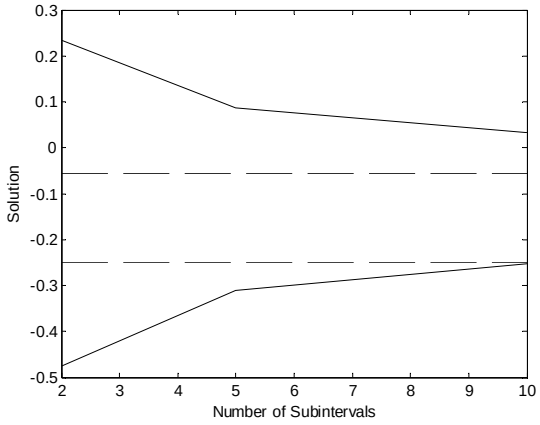

Figure 13.16. Behavior of the solution bounds with the number of subintervals for node 4 in the 12 element mesh.

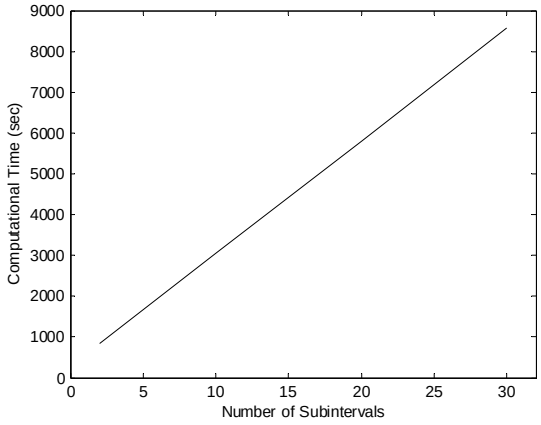

Figure 13.17. Computational cost with the number of subintervals for the 36 element mesh.

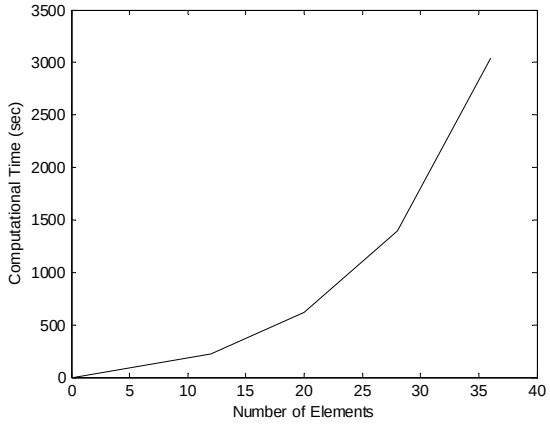

Figure 13.18. Computational cost of IBEM with mesh refinement using 10 subintervals.

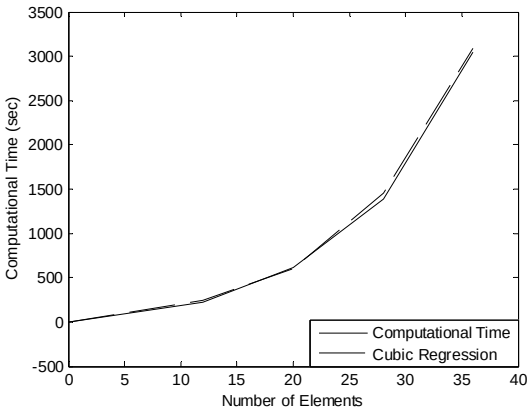

Figure 13.19. Computational cost with mesh refinement and cubic regression.

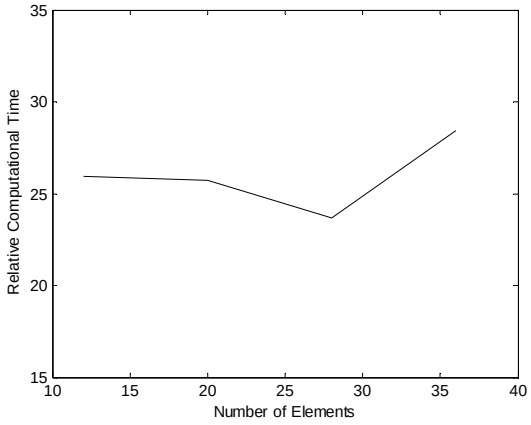

Figure 13.20. Ratio of the IBEM computational time, using 10 subintervals, to the conventional BEM computational time.

The sixth example demonstrates the behavior of the solution bounds to the Laplace equation for the the L-shaped domain (Figure 13.21). The temperature boundary conditions that are applied at all edges satisfy the Laplace equation as:

$$\left.\begin{array}{l} \nabla^2 u = 0 \quad in\ \Omega \\ u = \sinh(x)\sin(y) \quad on\ \Gamma \end{array}\right\}$$

Four different uniformly spaced meshes consisting of 6, 12, 18, and 24 elements with the node numbering starting in the bottom left corner and increasing counter clockwise (Figure 13.21) are considered.

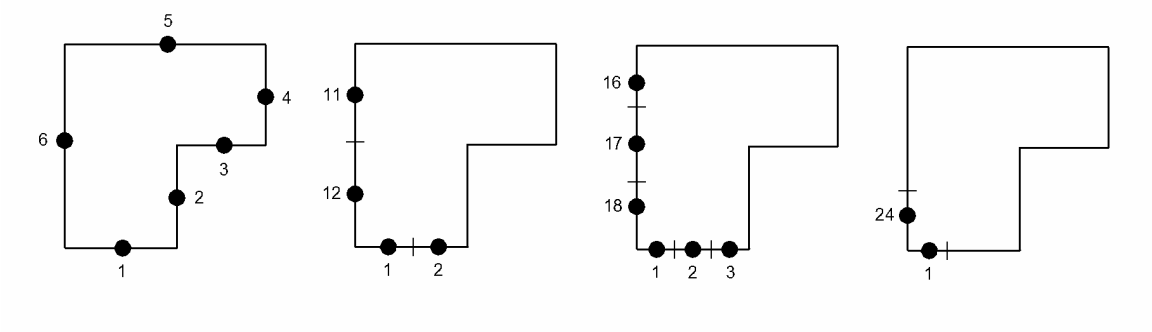

Figure 13.21. Boundary discretization of the L-shaped domain using constant boundary elements.

Ten equally spaced subintervals were chosen for parameterization since parameterization in terms of more subintervals did not yield much improvement in the solution. The results for the different meshes are compared at the left bottom elements 6, 12, 18, and 24 (Figure 13.21) for the respective meshes. Figure 13.22, Figure 13.23, and Figure 13.24 show the behavior of the solution width, effectivity index, and solution bounds, respectively, for these elements with decreasing element size. The interval solution is depicted with a solid line and the true solution is depicted with a dashed line. Figure 13.25 illustrates the behavior of the solution bounds for the left edge for the different meshes considered, solid line, and is compared with the true solution, dashed line. The behavior of the discretization error width with number of subintervals is shown (Figure 13.26) where number of subintervals increases from left to right and from top to bottom. The system is analyzed for 2, 5, 10, and 20 subintervals.

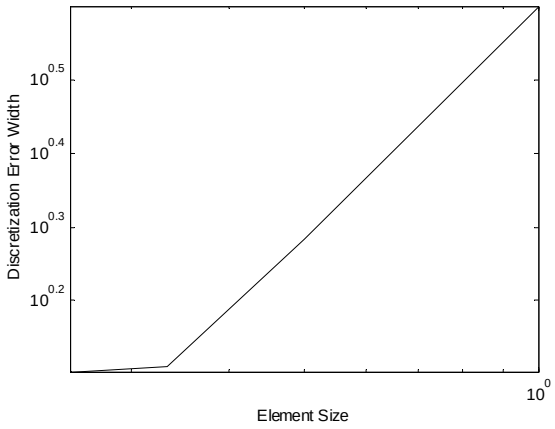

Figure 13.22. Behavior of the solution width with problem size.

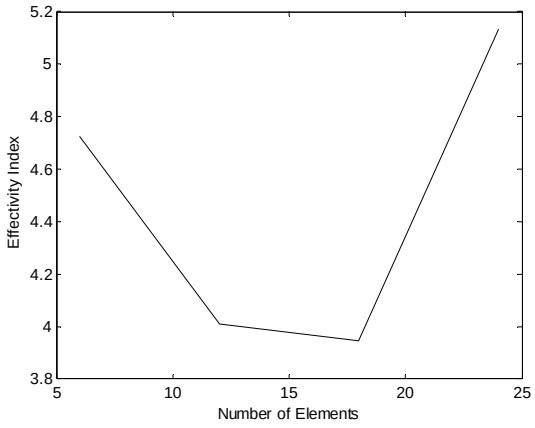

Figure 13.23. Behavior of the effectivity index with problem size.

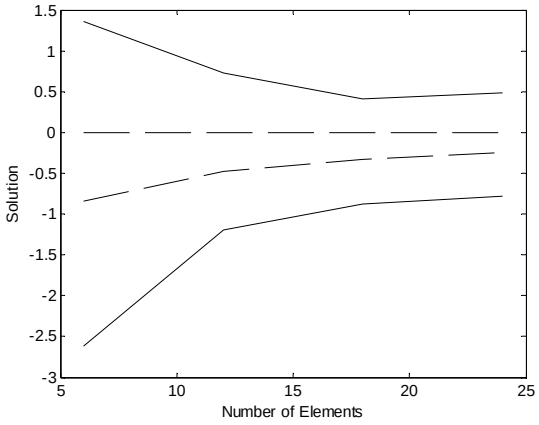

Figure 13.24. Behavior of the solution bounds with problem size.

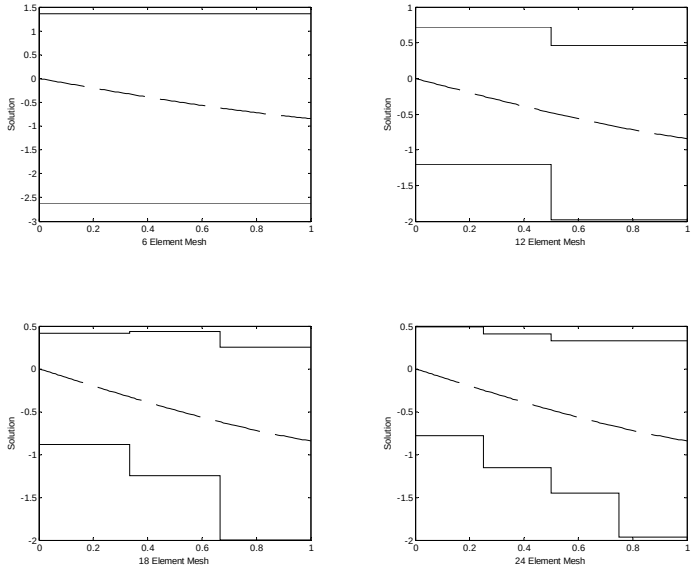

Figure 13.25. Behavior of the interval bounds for the different meshes on the left edge.

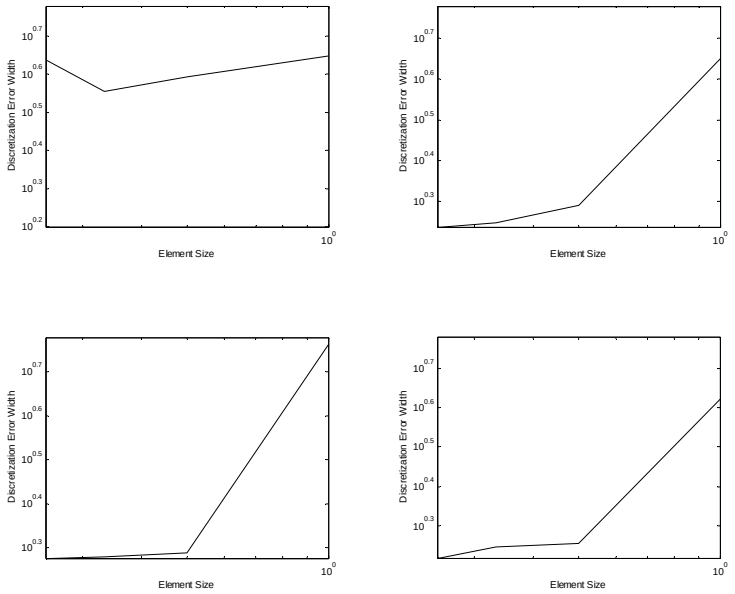

Figure 13.26. Behavior of the discretization error for different number of subintervals.

13.5 Discretization Error Analysis Using Interval Boundary Element Method for an Elasticity Problem

The seventh example obtains the bounds on the discretization error for the BEA of the elasticity problem. A unit square domain with zero traction on each side is considered as well as a zero displacement on the bottom, a zero displacement in the x direction on the top, and a unit displacement in the y direction on the top. Four different meshes (Figure 13.26) are considered and analyzed using 10 subintervals.

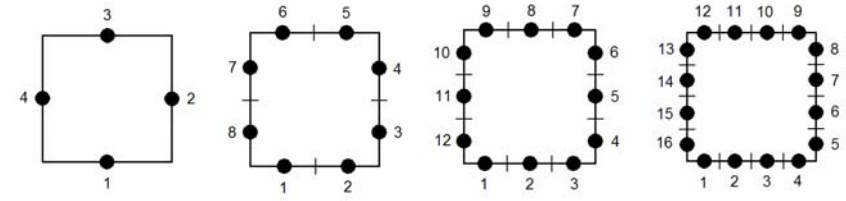

Figure 13.27. Constant boundary element discretization.

The behavior of the solution width, effectivity index, and the interval bounds on the true solution for nodes 2, 3, 4, 5, for the five respective meshes, is shown (Figure 13.27, Figure 13.28, Figure 13.29). The interval solution is shown by solid lines and the true solution by a dashed line. The behavior of the interval bounds for the right edge with mesh refinement is shown, solid line, and compared with the true solution, dashed line (Figure 13.30).

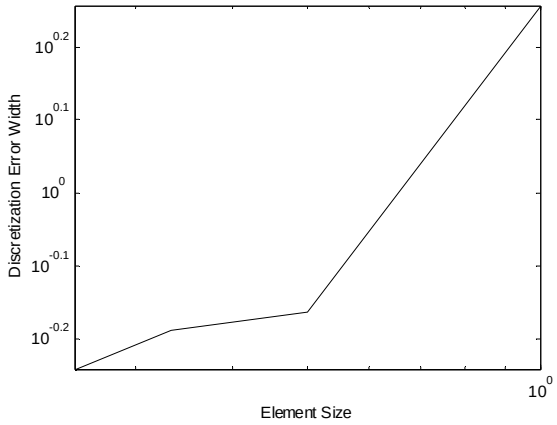

Figure 13.28. Behavior of the solution width with problem size.

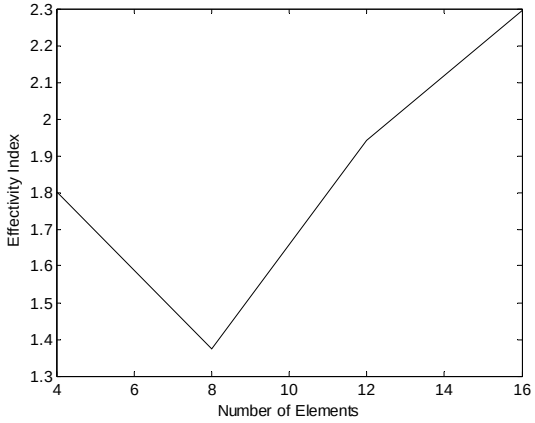

Figure 13.29. Behavior of the effectivity index with problem size.

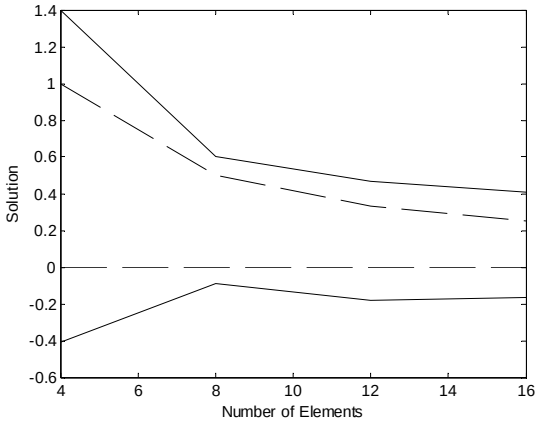

Figure 13.30. Behavior of the solution bounds with problem size.

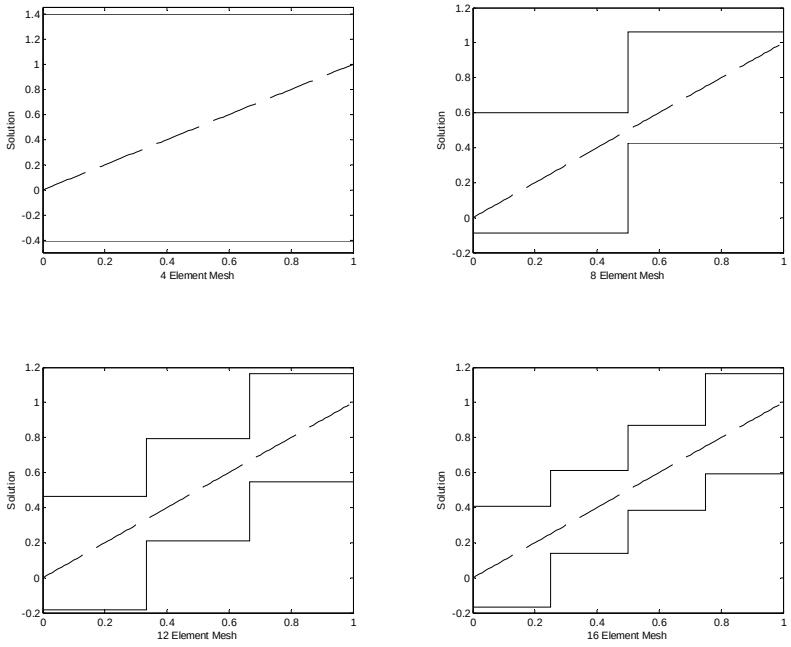

Figure 13.31. Behavior of the solution bounds for the different meshes for the right edge.

The eighth example solves the problem of hexagonal plate in tension (Figure 13.31). A positive unit displacement in the y direction is applied at the top of the plate and a negative unit displacement in the y direction is applied at the bottom of the plate.

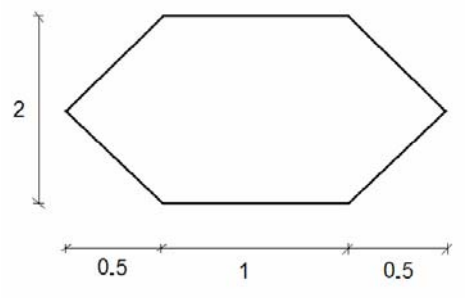

Figure 13.32. Hexagonal plate in tension.

A symmetry model is considered with a unit displacement at the top, to decrease the computational time, and is discretized using constant boundary elements (Figure 13.32, Figure 13.33). Ten subintervals are used in the computation.

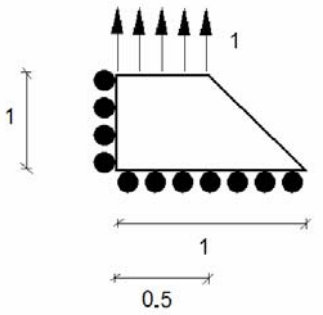

Figure 13.33. Symmetry model of the hexagonal plate.

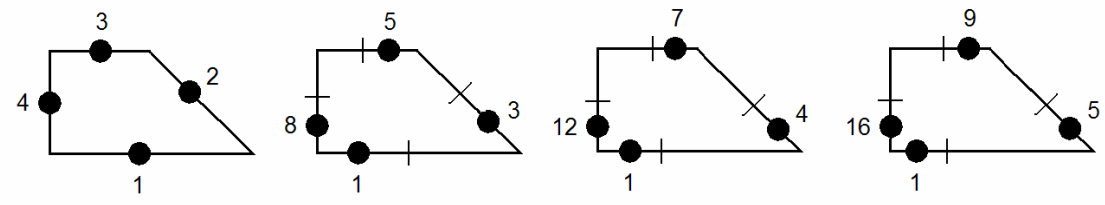

Figure 13.34. Boundary discretization using constant elements.

The behavior of the solution width, effectivity index, and solution bounds is depicted (Figure 13.34, Figure 13.35, Figure 13.36) for the displacement in the y direction for nodes 4, 8, 12, and 16 for the four respective meshes (Figure 13.33). The interval bounds, depicted by a solid line bounding the dashed true solution for the left edge displacement in the y direction are shown (Figure 13.37).

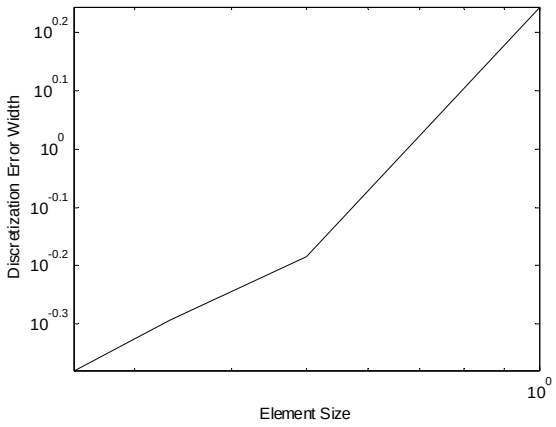

Figure 13.35. Behavior of the solution width with problem size.

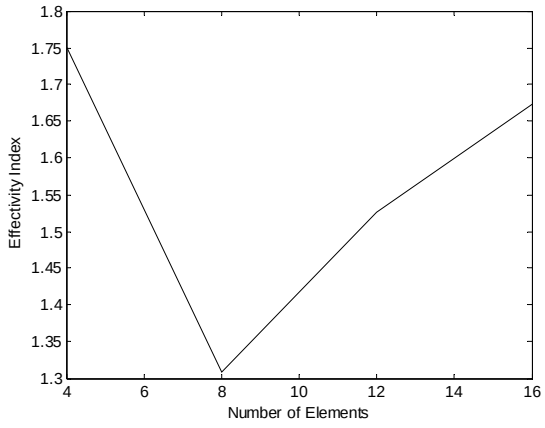

Figure 13.36. Behavior of the effectivity index with problem size.

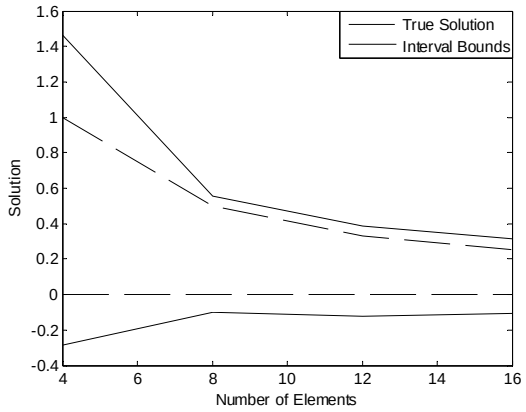

Figure 13.37. Behavior of the solution bounds with problem size.

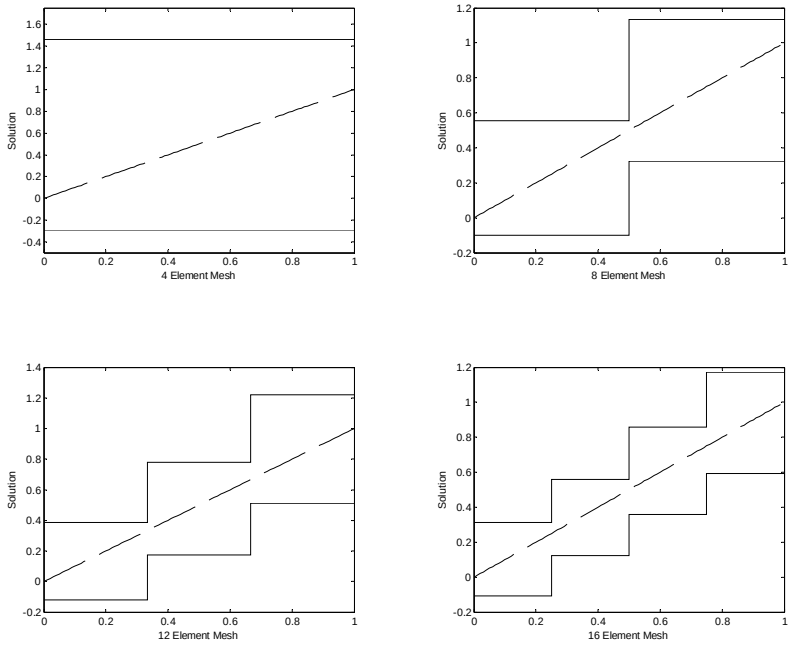

Figure 13.38. Behavior of the solution bounds for the different meshes for the left edge.

13.6 Discretization Error Analysis Using Interval Boundary Element Method for a Laplace Equation with Flux Singularities

The ninth example demonstrates the treatment of the discretization error for a Laplace equation with a geometrically induced flux singularity. A unit square domain with boundary conditions satisfying Laplace equation is considered (Figure 13.38). In order to compute effectivity indices the exact solution to the Laplace equation was chosen as:

$$\left.\begin{array}{l} \nabla^2 u = 0 \ in \Omega \\ u = \sqrt{\sqrt{(x-0.5)^2 + y^2}} \sin\left[\frac{1}{2}\arccos\left(\frac{x-0.5}{\sqrt{(x-0.5)^2 + y^2}}\right)\right] on \Gamma_1 \end{array}\right\}$$

with a singularity located at $x = \frac{1}{2,}\ y = 0$ which is depicted by a symbol ✳ (Figure 13.38). The temperature boundary conditions were applied on elements 2 and 4 for the five element mesh and the heat flux boundary conditions were applied on elements 1, 3, and 5 for the five element mesh. For the remaining meshes the temperature and heat flux boundary conditions were applied on the same boundaries as for the five element mesh.

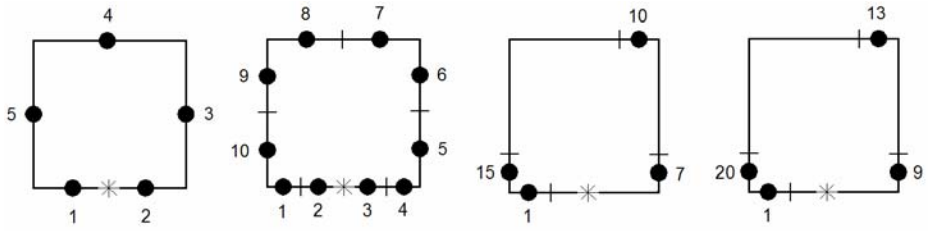

Figure 13.39. Boundary discretization using constant boundary elements.

Twenty equally spaced subintervals were chosen for parameterization since parameterization in terms of more subintervals did not yield much improvement in the

solution. The solution width and the effectivity indices are compared for the different meshes at the right bottom elements 3, 5, 7, and 9 (Figure 13.39, Figure 13.40) for the respective meshes. Figure 13.41 shows the behavior of the solution bounds for these elements with decreasing element size, solid line, compared with the true solution, dashed line. Figure 13.42 depicts the interval bounds, solid line, of the heat flux intensity factor, dashed line, for elements 2, 3, 4, and 5 for the four respective meshes. Figure 13.43 and Figure 13.44 illustrate the behavior of the interval bounds, solid line, compared with the true solution, dashed line, for right bottom elements 3, 5, 7, 9, for the four respective meshes and the behavior of the effectivity index with increased parameterization. Figure 13.45 depicts the interval bounds, solid line, compared with the true solution, dashed line, for the potential solution for the right edge with increasing number of elements.

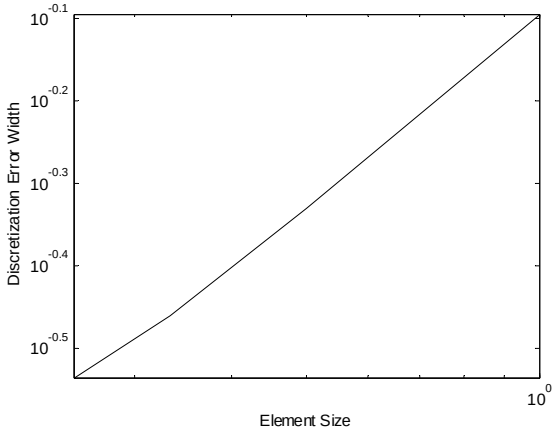

Figure 13.40. Behavior of the solution width with problem size.

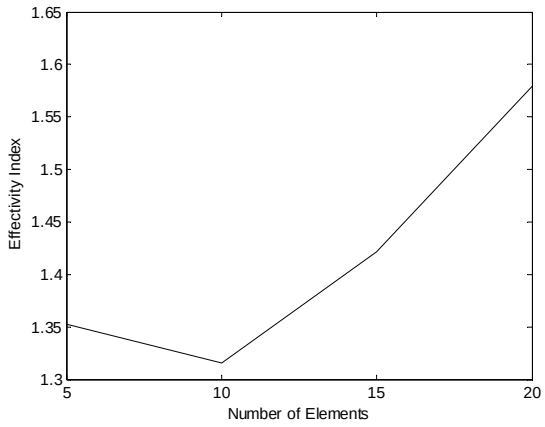

Figure 13.41. Behavior of the effectivity index with problem size.

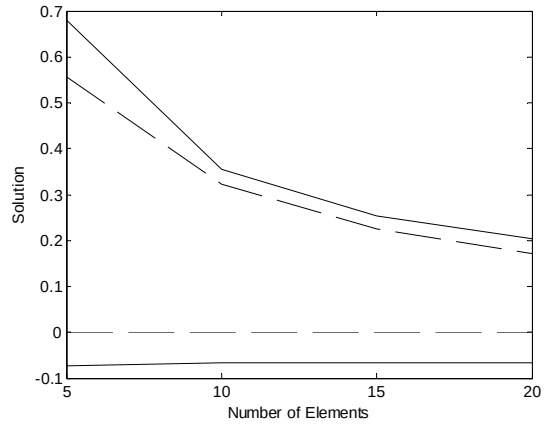

Figure 13.42. Behavior of the solution bounds with problem size.

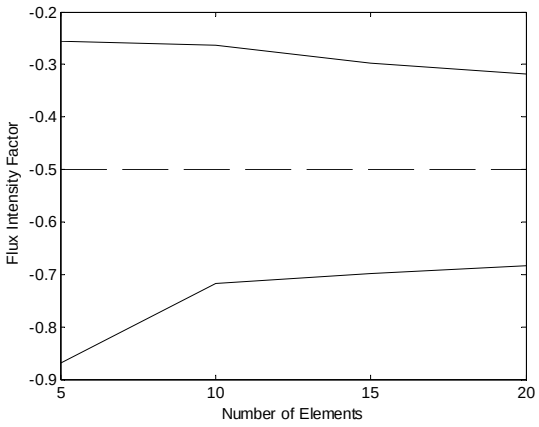

Figure 13.43. Behavior of the bounds on the heat flux intensity factor for the different meshes.

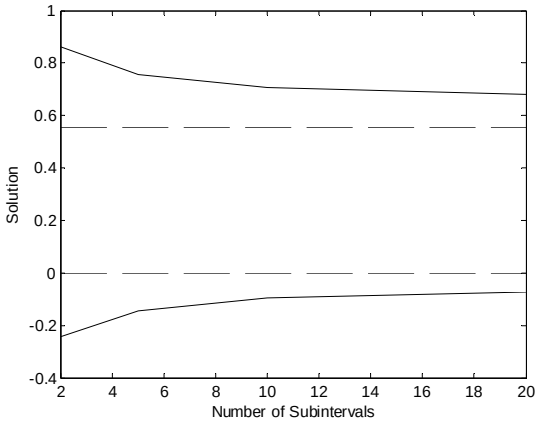

Figure 13.44. Behavior of the solution bounds with the number of subintervals.

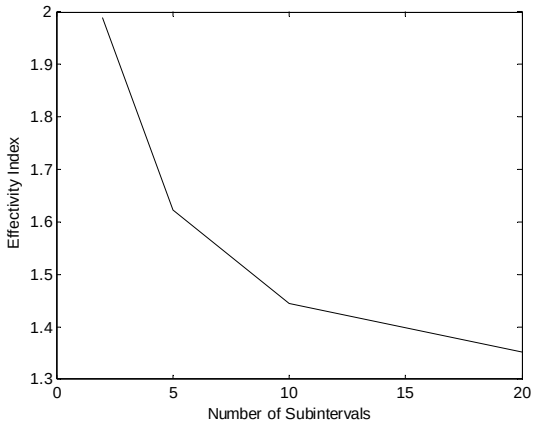

Figure 13.45. Behavior of the effectivity index with the number of subintervals.

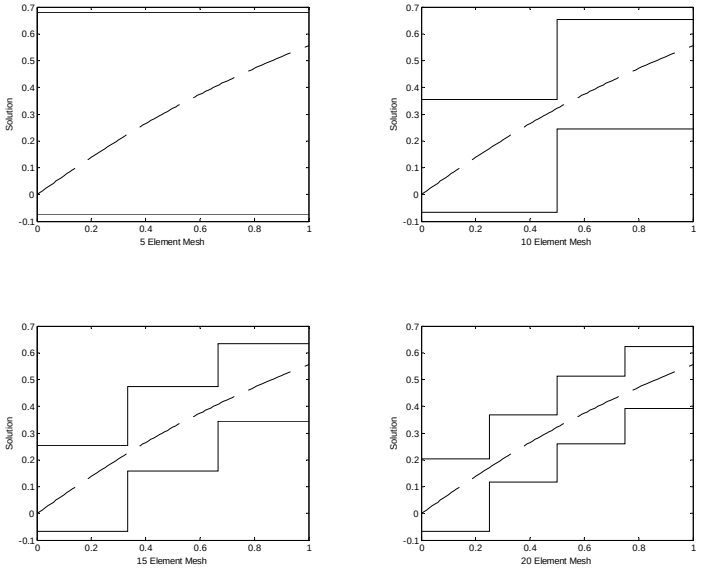

Figure 13.46. Behavior of the interval bounds for the different meshes for the right edge.

Chapter XIV: Research Conclusions

Chapter XIV provides conclusions on the present work and behavior of IBEM.

14.1 Concluding Remarks on the Interval Boundary Element Method

The objective in the development of the interval boundary element method (IBEM) was to provide a reliable engineering computing method that is capable of treating errors and uncertainties in an integrated and elegant fashion while being computationally efficient. IBEM is capable of treating the uncertainty in boundary conditions as well as errors occurring from numerical integration, floating point number truncation, and discretization of the integral equation. Moreover, IBEM enables computations of guaranteed solutions on the design variable level, a characteristic especially important in design engineering. The developed method is general and can be used to solve any linear elliptic partial differential equation, whose Green's function is known, for geometry of any complexity. Although, only two dimensional problems were analyzed for illustrative purposes, the extension of the work to three dimensions can be made following the presented methodology. The numerical examples have shown the efficiency of the method in terms of its convergence and computational time. From the examples presented, it can be noted that the interval solutions converge to the true solution with mesh refinement. The interval bounds are also decreased by increasing parameterization, which is essential in solving the discretization error problem. The computational cost of parameterization is roughly linear and therefore very efficient. In

general, besides the fourth example in chapter XIII, the effectivity index of the discretization error was shown to increase with mesh refinement, which is uncharacteristic for the discretization error. The overestimation in the discretization error bounds occurs due to several aspects inherent in interval computations. The first one is the interval enclosure of the boundary integral equation using the developed interval kernel splitting technique (IKST). Using IKST, one of the kernel functions is enclosed by its minimum and maximum bounds such that the subdistributive property is not violated. Unless the function is a constant, enclosing the kernel in such a way overestimates the enclosure and the resulting integral of the bounded kernel. The second reason for the overestimation of the discretization error is the incapability of the correct parameterization of the system. The kernel functions are nonlinear functions of the location of the source point, and therefore, subdivision of the entire interval, which encloses all possible locations of the source point, into subintervals is performed. This subdivision, does not allow for the perfect dependency of the location of the source point on any individual element unless infinite number of subintervals is considered, which of course is not possible. The third reason for the discretization error overestimation is the incomplete consideration of the subinterval parameterization within the developed solver. The interval solution, by problem definition, must be found on the entire element. Therefore, the subinterval bounds cannot be viewed entirely independent and must be considered as a union in interval operations. The fourth reason for the overestimation is inherent in solving an interval linear system of equations. The iterative schemes solve the problem in an orthogonal coordinate system defined by the user. In general, the interval

bounds are not orthogonal but rather hyper-ellipsoidal in multi-dimensions and the overestimation occurs in the corners of the enclosure (Figure 14.1).

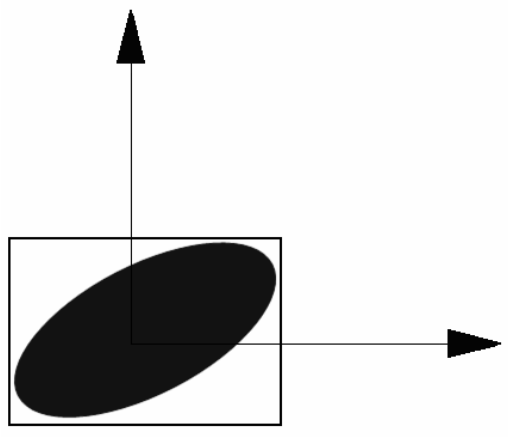

Figure 14.1. Interval bounds on the solution.

Also, in general, the true set is not aligned with the prescribed coordinate system. Large overestimations can occur especially if the true solution is longer in one direction, which is not aligned with the chosen coordinate system. Because there are many variables to consider, it is impossible to consider all the coordinate systems to achieve a better enclosure (Figure 14.2).

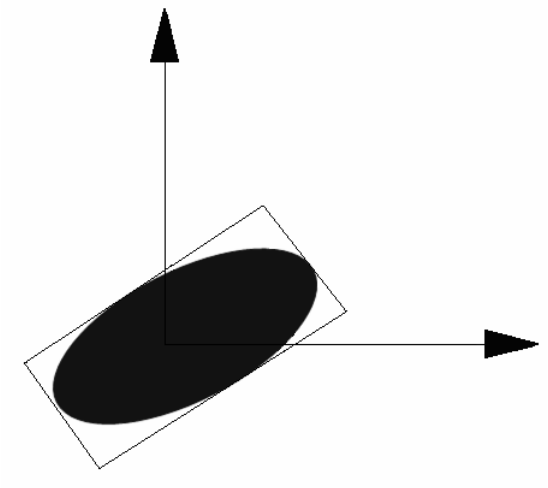

Figure 14.2. Rotated interval bounds on the solution.

For very small systems, where this optimal coordinate system can be found (Figure 14.2), and therefore sharper bounds can be obtained in that coordinate system, this preferred coordinate system is of little use since the transformation of the interval bounds to a more useful, original, coordinate system would impose the same, if not worse, overestimation (Figure 14.3).

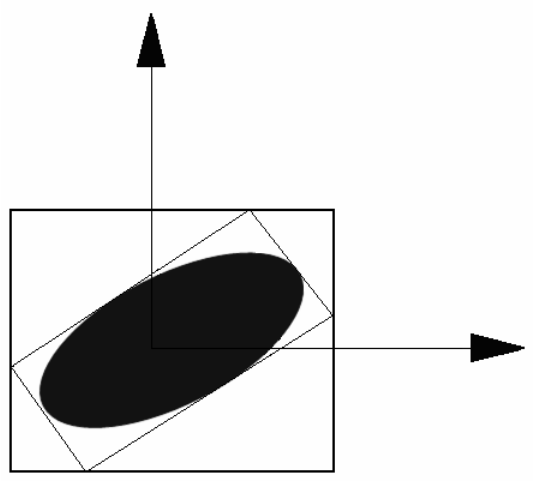

Figure 14.3. Transformed interval bounds on the solution.

Hence, the interval solution has a slower convergence rate than the true solution, which is the cumulative reason for the increasing effectivity index. The discretization error bounds for the variables in the interior of the domain are shown to decrease with mesh refinement. The interior error bounds assume correct error bounds on the boundary of the system and their computation itself does not provide any additional overestimation. For problems with geometrically induced flux singularities, IBEM is capable of not only computing the discretization error bounds for all elements except the element on which the singularity is present, but also the bounds on the flux intensity factor for the singular flux element. The cost of the computation varies cubically with the number of elements

and is roughly equal to $2.5 \cdot \left(number\ of\ subintervals\right) \cdot \frac{\left(number\ of\ elements\right)^3}{constant}$. Therefore it is directly proportional, by $2.5 \cdot \left(number\ of\ subintervals\right)$, to the cost of the conventional BEA for a particular mesh. IBEM is also capable of enclosing the true solution in presence of integration and rounding errors. The rounding error bounds can be easily incorporated into the solver of interval linear system of equations. The solutions in presence of integration error have been enclosed and although the procedure was demonstrated on the Taylor series expansion, other numerical integration schemes can be used following the same methodology. The behavior of the solution bounds will depend on the method of numerical integration. The uncertainty in boundary conditions has been treated using an interval approach. The solutions of IBEM with interval uncertainty in the applied boundary conditions only, are exact and therefore independent of the problem size. As the uncertainty in the boundary conditions most likely produces the largest level of uncertainty in the solutions, IBEM is a very attractive tool for these types of computations.

Bibliography

Alefeld, G. and Herzberger, J., *Introduction to Interval Computations*, Academic Press, New York, NY, 1983.

Aliabadi, M. H., *The Boundary Element Method Vol. 2: Applications in Solids and Structures*, John Wiley and Sons, LTD., West Sussex, 2002.

Archimedes of Syracuse, *The Works of Archimedes Translated by Sir Thomas Health*, University Press, Cambridge, 1897.

Babuška, I., Nobile, F., and Tempone, R., Reliability of Computational Science, *Numerical Methods for Partial Differential Equations*, Vol. 23 (4), pp. 753-784, 2007.

Babuška, I. and Stroubolis, T., *The Finite Element Method and Its Reliability*, Clarendon Press, Oxford, 2001.

Babuška, I., Zienkiewicz, O. C., Cago, J., and Oliveira E. R. deA., *Accuracy Estimates and Adaptive Refinements in Finite Element Computations*, John Wiley and Sons, LTD., India, 1986.

Banerjee P. K. and Watson, J. O., *Developments in Boundary Element Methods – 4*, Elsevier Applied Science Publishers, London, 1986.

Beskos, D. E., *Boundary Element Methods in Structural Analysis*, ASCE, 1989.

Blandford, G. E., Ingraffea A. R., and Liggett, J. A., Two-Dimensional Stress Intensity Factor Computations Using the Boundary Element Method, *International Journal for Numerical Methods in Engineering*, Vol. 17, pp. 387-404, 1981.

Brebbia, C. A. and Dominguez, J., Boundary Element Method for Potential Problems, *Applied Mathematical Modeling*, Vol. 1, pp. 372-378, 1977.

Brebbia, C. A., *The Boundary Element Method for Engineers*, John Wiley & Sons, New York, 1978.

Brebbia, C. A., Futagami, T., and Tanaka, M., Boundary Elements, Proceedings of the Fifth International Conference, Hiroshima, Japan, November, 1983.

Brebbia, C. A. and Dominguez, J., *Boundary Elements: An Introductory Course*, Computational Mechanics, New York, McGraw-Hill, 1992.

Bronsztejn, L. N. and Siemiendiajew, K. A., *Matematyka: Poradnik Encyklopedyczny Vol. 3*, Panstwowe Wydawnictwo Naukowe, Warsaw, 1968.

Bronsztejn, L. N. and Siemiendiajew, K. A., *Matematyka: Poradnik Encyklopedyczny Vol. 4*, Panstwowe Wydawnictwo Naukowe, Warsaw, 1970.

Burczynski, T. and Skrzypczyk, J., Fuzzy Aspects of the Boundary Element Method, *Engineering Analysis with Boundary Elements*, Vol. 19, pp. 209-216, 1997.

Cartensen, C. and Stephan E. P., A Posteriori Error Estimates for Boundary Element Method, *Mathematics of Computations*, Vol. 64, No. 210, pp. 483-500, 1995.

Collins, G., *Interval Arithmetic for Automatic Error Analysis*, M&A-5, Mathematics and Applications Department, IBM, 1960.

Cruse, T. A., *Boundary Element Analysis in Computational Fracture Mechanics*, Kluwer Academic Publishers, Dordrecht, The Netherlands, 1988.

Dehao, Y. and Lonhgua, Z., Boundary Integral Equations and A Posteriori Error Estimates, *Engineering Analysis with Boundary Elements*, Vol. 10, pp. 35-42, 2005.

Dennis Jr., J. E. and Schnabel, R. B., *Numerical Methods for Unconstrained Optimization and Nonlinear Equations*, SIAM, Philadelphia, 1996.

Dobner, H., Kernel-Splitting Technique for Enclosing the Solution of Fredholm Equations of the First Kind, *Reliable Computing*, Vol. 8, pp. 469-179, 2002.

Dwyer, P. S., *Linear Computations*, J. Wiley, N.Y., 1951.

Dwyer, P. S., Matrix inversion with the square root method, *Technometrices*, Vol. 6, 2, pp. 197-213, 1964.

Fenner, R. T., *Engineering Elasticity Application of Numerical and Analytical Techniques*, John Wiley & Sons, New York, 1986.

Fredholm, I., Su Rune Classe D'equations Functionalles, *Acta Mathematica*, Vol. 27, pp. 365-390, 1903.

Friedman, A., *Partial Differential Equations***,** R. E. Krieger Pub. Co., Huntington, N.Y., 1976.

Gaul, L., Boundary Element Method, Class Notes, Institut für Angewandte und Experimentelle Mechanik, http://www.iam.uni-stuttgart.de/bem/.

Gay, D. M., Solving Interval Linear Equations, *SIAM Journal on Numerical Analysis*, Vol. 19, 4, pp. 858-870, 1982.

Goos, G. and Hartmanis, J., Interval Mathematics 1985, *Proceedings of the International Symposium Freiburg i. Br.*, Federal Republic of Germany, September 23-26, 1985.

Hall, W. S., *The Boundary Element Method*, Kluwar Academic Publishers, Boston, 1994.

Hammersley J. M. and Handscomb D. C., *Monte Carlo Methods*, Chapman and Hall, London & New York, 1964.

Hansen, E., Interval Arithmetic in Matrix Computation, *J. S. I. A. M., series B, Numerical Analysis*, part I, 2, 308-320, 1965.

Hansen, E., A Globally Convergent Interval Method for Computing and Bounding Real Roots, *BIT*, Vol. 18, pp. 415-424, 1978.

Hartmann, F., *Introduction to Boundary Elements: Theory and Applications*, New York, Springer-Verlag, 1989.

Huang, Q. and Cruse, T. A., Some Notes On Singular Integral Techniques In Boundary Element Analysis, *International Journal for Numerical Methods in Engineering*, Vol. 36, pp. 2643-2659, 1993.

Huang, C-S., Lee, C-F., and Cheng, A. H-D., Error Estimate, Optimal Shape Factor, and High Precision Computation of Multiquadric Collocation Method, *Engineering Analysis with Boundary Elements*, Vol. 31, pp. 614-623, 2007.

Jansson, C., Interval Linear System with Symmetric Matrices, Skew-Symmetric Matrices, and Dependencies in the Right Hand Side, *Computing*, Vol. 46, pp. 265-274, 1991.

Jaswon, M. A. and Symm, G. T., *Integral Equation Methods in Potential Theory and Elastostatics*, Academic Press, London, 1977.

Jou, J. and Liu, J., A Posteriori Boundary Element Error Estimation, *Journal of Computational and Applied Mathematics*, Vol. 106, pp. 1-19, 1999.

Kearfott, R. B., Preconditioners For the Interval Gauss-Seidel Method, *SIAM Journal of Numerical Analysis*, Vol. 27, No. 3, pp. 804-822, 1990.

Kellogg, O. D., *Foundations of Potential Theory*, Springer, Berlin, 1929.

Krawczyk, R., Newton-Algorithmen zur Bestimmung von Nullstellen mit Fehlerschranken, *Computing*, Vol. 4, pp. 187-201, 1969.

Kupradze, V. D., *Potential Methods in the Theory of Elasticity*, Israel Programme for Scientific Translations, Jerusalem, 1965.

Lax, P. D. and Milgram, A. N., Parabolic Equations, Annals of Mathematics Studies, Vol. 33, pp. 167-190, 1954.

Liggett, A. J. and Liu, Philip, L-F. *The Boundary Integral Equation Method for Porous Media Flow*, George Allen & Unwin, London, 1983.

Linkov, A. M. *The Boundary Integral Equations in Elasticity Theory*, Kluwer Academic Publishers, London, 2002.

Liu, G. R. *Mesh Free Methods, Moving Beyond the Finite Element Method*, CRC Press, London, 2003.

MATLAB 6.5.1., *Using Matlab Version 6 OEM Manual the Language of Technical Computing*, Mathworks, 2002.

Mikhlin, S. G., *Multidimensional Singular Integrals and Integral Equations*, Pergamon Press, Oxford, 1965.

Modares, M. and Mullen, R. L., Free Vibration of Structures with Interval Uncertainty, *9th ASCE Specialty Conference on Probabilistic Mechanics and Structural Reliability*, 2004.

Modares, M., Mullen, R. L., Bellini, P. X., and Muhanna, R. L., Buckling Analysis of Structures with Interval Parameters, *Proceeding of the 2005 SAE World Congress, Reliability and Robust Design in Automotive Engineering*, Detroit, Michigan, April 11-14, 2005.

Moore, R. E., *Interval Arithmetic and Automatic Error Analysis in Digital Computing*, Ph. D. Dissertation, Stanford University, 1962.

Moore, R. E., *Interval Analysis*, Prentice-Hall, Inc., Englewood Cliffs, N. J, 1966.

Muhanna, R. L. and Mullen, R. L., Development of Interval Based Methods for Fuzziness in Continuum Mechanics, *Proceedings of ISUMA-NAFIPS '95*, IEEE Computer Society Press, Los Alamos, California, pp. 145-150, 1995.

Muhanna, R. L. and Mullen, R. L., Formulation of Fuzzy Finite Element Methods for Mechanics Problems, *Computer Aided Civil and Infrastructure Engineering*, Vol. 14, pp. 107-117, 1999.

Muhanna, R. L. and Mullen, R. L., Uncertainty in Mechanics Problems - Interval-Based Approach, *Journal of Engineering Mechanics*, ASCE, Vol. 127, No. 6, pp. 557-566, 2001.

Muhanna, R. L., Mullen, R. L., and Zhang, H., Penalty-Based Solution for the Interval Finite Element Methods, *Journal of Engineering Mechanics*, ASCE, Vol. 131, No. 10, pp 1102-1111, 2005.

Mullen, R. L. and Rencis, J. J., Iterative Methods for Solving Boundary Element Equations, *Computers and Structures*, Vol. 25 (5), pp. 713- 723, 1987.

Mullen, R. L. and Muhanna, R. L., Structural Analysis with Fuzzy-Based Load Uncertainty, *Proceedings of 7th ASCE EMD/STD Special Conference on Probabilistic Mechanics and Structural Reliability*, WPI, MA, ASCE, New York, pp. 310-313, 1995.

Mullen, R. L. and Muhanna, R. L., Interval-Based Finite Element Methods, *Reliable Computing*, 5 pp. 97-100, 1999.

Mullen, R. L. and Muhanna, R. L., Bounds of Structural Response for All Possible Loadings, *Journal of Structural Engineering, ASCE*, Vol. 125, No. 1, pp. 98-106, 1999.

Mullen, R. L. and Muhanna, R. L., Efficient Interval Methods for Finite Element Solution, *Proceedings of the 16th Annual International Symposium on High Performance Computing Systems and Applications*, 2002.

Neumaier, A., Overestimation in Linear Interval Equations, *SIAM Journal on Numerical Analysis*, Vol. 24, 1, pp. 207-214, 1987.

Neumaier, A., Rigorous Sensitivity Analysis for Parameter-Dependent Systems of Equations, *Journal of Mathematical Analysis and Applications*, Vol. 144, pp. 16-25, 1989.

Neumaier, A., *Interval Methods for Systems of Equations*, Cambridge University Press, 1990.

Neumaier, A. and Pownuk, A., Linear Systems with Large Uncertainties, with Applications to Truss Structures, *Reliable Computing*, Vol. 13, pp. 149-172, 2007.

Neumaier, A., Certified Error Bounds for Uncertain Elliptic Equations, *Journal of Computational Applied Mathematics*, 2007, in review.

Oden, J. T. and Carey, G. F., *Finite Elements: Mathematical Aspects, Volume 4*, Prentice Hall, 1983.

Oden, J. T. and Prudhomme, S., Goal-Oriented Error Estimation and Adaptivity for the Finite Element Method, *Computers and Mathematics with Applications*, Vol. 41, pp. 735-756, 2001.

Ostrowski A., Recherches Sur la Methode de Graeffe et les Seros des Polynomes et des Series des Laurent, *Acta Mathematica*, Vol. 72, pp. 99-257, 1940.

Piasecka Belkhayat, A., Interval Boundary Element Method for 2D Transient Diffusion Problem, *Engineering Analysis with Boundary Elements*, 2007, in press.

Pilkey, W. D. and Wunderlich W., *Mechanics of Structures, Variation and Computational Methods*, CRS Press, London, 1994.

Rencis, J. J. and Mullen, R. L., Solution of Elasticity Problems by a Self-Adaptive Mesh Refinement Technique for Boundary Element Computation, *International Journal for Numerical Methods in Engineering*, Vol. 23, pp. 1509-1527, 1986.

Rencis, J. J. and Mullen, R. L., Self-Adaptive Mesh Refinement for Boundary Element Solutions of Laplace Equation, *Computational Mechanics*, Vol. 3, pp. 309-319, 1988.

Rencis, J. J. and Jong, K-Y., An Error Estimator for Boundary Element Computations, *ASCE Journal of Engineering Mechanics*, Vol. 115, 9, pp. 1993-2010, 1989.

Rizzo F. J., An Interval Equation Approach to Boundary Value Problems of Classical Elastostatics, *Quarterly of Applied Mathematics*, Vol. 25, pp. 83-95, 1967.

Ross, T. J., *Fuzzy Logic with Engineering Applications*, McGraw-Hill, Inc., New York, 1995.

Rump, S. M., *Kleine Fehleschranken bei Matrixproblem*, Ph. D. Dissertation, Universitat Karlsruhe, 1980.

Rump, S. M., Rigorous Sensitivity Analysis for Systems of Linear and Nonlinear Equations, *Mathematics of Computations*, Vol. 54, 190, pp. 721-736, 1990.

Rump, S. M., On the Solutions of Interval Systems, *Computing*, Vol. 47, pp. 337-353 1992.

Rump, S. M., Self-validating Methods, *Linear Algebra and its Applications*, Vol. 324, pp. 3-13, 2001.

Saada, A. S. *Elasticity: Theory and Applications, Second Edition*. Krieger Publishing Co., Malabar, FL, 1993.

Samko, S. G., *Hypersingular Integrals and Their Applications*, Taylor & Francis, New York, 2002.

Sawada, T. and Imanari, M., Error Estimate of Numerical Integration in Boundary Element Method Analysis, *BULL. JSME*, Vol. 29, 258, pp. 4072-4079, 1986.

Shames, I. H. and Pitarresi, J. M., *Introduction to Solid Mechanics, Third Edition*. Prentice Hall, New Jersey, 2000.

Skalna, I. and Pownuk, A., On Using Global Optimization Method for Approximating Interval Hull Solution of Parametric Interval Systems, *Proceeding of the 2008 REC2008 Conference*, 2008.

Somigliana, C., Sopra L'equilibrio di us Corpo Elastico Isotropo, *Il Nuovo Ciemento*, tome 17-19, 1885.

Sunaga, T., Theory of interval algebra and its application to numerical analysis, *RAAG Memoirs 3*, pp 29-46, 1958.

Sweldow, J. L. and Cruse, T. A., Numerical Solutions in Three Dimensional Elastostatics, *International Journal of Solids and Structures*, Vol. 5, pp. 1259-1274, 1971.

Tanaka, M., Brebbia, C. A. And Shaw, R., *Advances in Boundary Elements Methods in Japan and USA*, Computational Mechanics Publications, Boston, 1990.

Taylor, B., *Methodus Incrementorum Directa & Inversa*, Londini, typis Pearsnianis, 1715.

Wrobel, L. C., *The Boundary Element Method Vol. 1: Applications in Thermo-Fluids and Acoustics*, John Wiley and Sons, LTD., West Sussex, 2002.

Zalewski, B. F., Mullen, R. L., and Muhanna, R. L., Boundary Element Analysis of Systems Using Interval Methods, *Proceeding of the 2006 REC2006 Conference*, 2006.

Zalewski, B. F. and Mullen, R. L., Discretization Error in Boundary Element Analysis using Interval Methods, *SAE 2007 Transactions Journal of Passenger Cars - Mechanical Systems*, Paper No. 2007-01-1482, 2007.

Zalewski, B. F., Mullen, R. L., and Muhanna, R. L., Interval Boundary Element Method in the Presence of Uncertain Boundary Conditions, Integration Errors, and Truncation Errors, *Engineering Analysis with Boundary Elements*, 2007, accepted.

Zalewski, B. F. and Mullen, R. L., Certified Bounds on Interval Fredholm Equations of the First and Second Kind, *Reliable Computing*, 2008, in review.

Zalewski, B. F. and Mullen, R. L., Point-wise Discretization Errors in Boundary Element Method for Elasticity Problem, *Proceeding of the 2008 REC2008 Conference*, 2008.

Zalewski, B. F. and Mullen, R. L., Interval Bounds on the Local Discretization Error in Boundary Element Analysis for Domains with Singular Flux, *SAE 2008 Reliability and Robust Design in Automotive Engineering*, Paper No. 2008-01-0707, 2008.

Zalewski, B. F. and Mullen, R. L., Interval Bounds on Local Discretization Error in Boundary Element Analysis of the Torsion Problem, *International Journal for Numerical Methods in Engineering*, 2008, in review.

Zienkiewicz, O. C., The Finite Element Method: Its Genesis and Future, *The Structural Engineer*, Vol. 70, No. 20, pp. 355-360, 1992.